Durham E-Theses

Identification of ubiquitin K33 and K48 as sites of CO2-dependent carbamylation with implications for intracellular CO2 signalling

PEGG, HAMISH,BENJAMIN

How to cite:

Use policy

Identification of ubiquitin K33 and K48 as sites of CO_2-dependent carbamylation with implications for intracellular CO_2 signalling

A thesis submitted for the degree of

Master of Science (MSc)

Hamish B. Pegg

Department of Biosciences

Durham University

2017

Abstract

CO_2 is a product of aerobic respiration that has been implicated in various signalling pathways in health and disease. However, the exact mechanisms of CO_2 signalling are poorly understood. This is due in large part to the lack of technology with which to study protein-CO_2 interactions, known as carbamylation, and thus identify CO_2 sensors. Recently a method for trapping carbamates, forming a carboxyethyl modification to the target residue, has been developed for downstream analysis of carbamate formation by MS. The aim of this thesis is to use this novel workflow to identify a CO_2 sensor. MALDI-TOF MS was performed to identify peptides containing carboxyethyl modification. LC-MS/MS was then performed to identify K33 and K48 as sites of carboxyethyl modification. These residues were demonstrated to be sites of carbamylation by introducing ^{13}C into the workflow. Finally, a cross-linking assay demonstrated CO_2-dependent reduction to the rate of ubiquitination. Together these results demonstrate two sites of carbamylation of ubiquitin with consequences to ubiquitination kinetics. Therefore, it is proposed that ubiquitin is a CO_2 sensor.

Declaration

The work presented in this thesis was carried out at Durham University between September 2016 and September 2017. The work is my own original research unless otherwise stated or indicated by citation. This work has not been submitted for any other qualification.

Statement of copyright

The copyright of this thesis rests with the author. No quotation from it should be published without the author's prior written consent and information derived from it should be acknowledged.

Acknowledgements

The work presented in this thesis was made possible by a large number of people.

I would first like to thank Prof. Martin Cann for his exemplary role as a supervisor, his enthusiasm and motivation for the project, and for the role he has played in shaping my future career. Dr Ehmke Pohl was a constant source of encouragement throughout this project and it was a privilege to have had him as a secondary supervisor.

I would like to thank Dr Adrian Brown for his mass spectrometry expertise and Prof Ari Sadanandom for his kind contribution of *pET30a UBQ11*. I would like to thank Dr Phil Townsend for sharing so much of his technical expertise with me. To Dr Vicki Linthwaite I am forever grateful you persisted with your PhD so that I might spend hours pouring over the pH Stat. For his training and permission to use the FPLC I would like to thank Dr Tim Blower, and for his advice and bad dad jokes I would like to thank Dr Gary Sharples.

To the members of 234 I would like to say a big thank you for your friendship and support. In particular I would like to thank Chris for his amusingly bleak assessment of the scientific world, Phil for his entertaining management of undergraduates, Vicki for being audible from anywhere in the building, Alex for his relentless desire to achieve maximum entropy on his bench, Tara for her constant encouragement and finally, Ale for her cheeriness even before the morning coffee break.

There are too many friends and family to say thank you to but you know who you are. Special shout outs to Jan for making Durham a thoroughly enjoyable place to live and to Kim for your encouragement throughout the thesis writing process.

Special thanks is reserved to Mum, Dad and Charlotte for their constant support and willingness to put up with a son/brother living too far away to visit home regularly.

Table of Contents

List of Figures

List of Tables

Abbreviations

A. thaliana	*Arabadopsis thaliana*
AMPK	AMP-activated protein kinase
ARDS	Acute respiratory distress syndrome
ATP	Adenosine triphosphate
CA	Carbonic anhydrase
cAMP	Cyclic adenosine monophosphate
CCL2	C-C motif chemokine 2
CFTR	Cystic fibrosis transmembrane conductance regulator
Cl^-	Chloride ion
CO_2	Carbon dioxide
COPD	Chronic obstructive pulmonary dysfunction
CORD	CO_2 responsive domain
Cx26	Connexin 26
Cx30	Connexin 30

Cx32	Connexin 32
Da	Dalton
DNA	Deoxyribonucleic acid
D. melanogaster	*Drosophila melanogaster*
DTT	Dithiothreitol
E1 ligase	E1 ubiquitin protein ligase
E2 ligase	E2 ubiquitin protein ligase
E2-25K	E2 ubiquitin protein ligase 25K
E3 ligase	E3 ubiquitin protein ligase
Gr63a	Gustatory and odorant receptor 63a
H^+	Hydrogen ion
HCO_3^-	Bicarbonate ion
HSF1	Heat shock factor 1
IL-6	Interleukin 6
IPTG	Isopropyl β-D-1-thiogalactopyranoside

iTRAQ	Isobaric tags for relative and absolute quantitation
IκB	NFκB inhibitor
JNK	Stress activated protein kinase JNK
K^+	Potassium ion
Kir	Kir 6.2 ATP-sensitive inward rectifier potassium channel
LC	Liquid chromatography
LC-MS/MS	Liquid chromatography tandem mass spectrometry
MALDI-TOF	Matrix assisted laser absorption onization time of flight
mE1	Mouse E1 ubiquitin protein ligase
MS	Mass Spectrometry
MS2	Tandem mass spectrometry
MuRF1	Muscle RING finger 1
MW	Molecular weight
Na^+	Sodium ion
NBC	Na^+/HCO_3^- cotransporter

NFκB	Nuclear factor κ B
NMR	Nuclear magnetic resonance
p100	NFκB subunit p100
p105	NFκB subunit 105
p50	NFκB subunit p50
p52	NFκB subunit p52
PKA	Protein kinase A
PKC	Protein kinase C
PTM	Post translational modification
RelB	Transcription factor RelB
RuBisCO	Ribulose-1,5-bisphosphate carboxylase/oxygenase
SCF	SKP1-CUL1-F-box protein
SDS-PAGE	Sodium dodecyl sulfate-polyacrylamide gel electrophoresis
SILAC	Stable isotope labeling with amino acids in cell culture
$NaHCO_3$	$NaHCO_3$ Sodium bicarbonate

TEO   Triethyloxonium tetrafluoroborate

TMT   Tandem mass tag

Zfh   Zinc finger homeobox protein (*Drosophila melanogaster*)

ZFHX   Zinc finger homeobox protein (*Homo sapiens*)

1. Introduction

1.1. Overview

Carbon dioxide (CO_2) is a primary product of oxidative metabolism that was first discovered by Joseph Black in the 18th century and has since been implicated in several human diseases (Cummins et al., 2014; West, 2014). Fundamentally, CO_2 has effects on respiration, photosynthesis, and acid-base homeostasis (Gutknecht et al., 1977; Hetherington and Raven, 2005; Joshi and Tabita, 1996). It readily dissolves into cells due to its hydrophobic properties, whereupon it becomes hydrated to form carbonic acid. Carbonic acid readily dissociates into HCO_3^- and H^+, thus linking the concentration of CO_2 in a cell to the pH (Blombach and Takors, 2015; Boron et al., 2011). CO_2 hydration occurs relatively slowly at physiological pH and is therefore the rate limiting step in the equilibrium (Khalifah, 1973). In order to overcome this carbonic anhydrase catalyses the hydration of CO_2. CAs are efficient enzymes with high turnover rates (Frommer, 2010; Lindskog, 1997). Their biological importance is demonstrated by their evolutionary conservation in all kingdoms of life (Moroney et al., 2001; Supuran et al., 2003). This suggests the ability to sense and respond to changes in CO_2 is an important homeostatic mechanism. However, this is a poorly understood area of cell biology and this thesis aims to better understand CO_2 sensing. Therefore, the focus of this thesis is CO_2 signalling and its direct interaction with proteins.

1.2. Carbamylation

The direct interaction of CO_2 with proteins results in a labile post translational modification (PTM), which is referred to in the literature with a range of definitions (e.g. carbamate, carbamino adduct, carboxylate). Herein, it is referred to as a carbamate. The reaction resulting in a carbamate, termed carbamylation, occurs between aqueous CO_2 and uncharged amine groups on proteins (Figure 1.1).

Carbamylation changes the electrochemical properties of the modified protein. This in turn alters the possible interactions and therefore function of the modified protein.
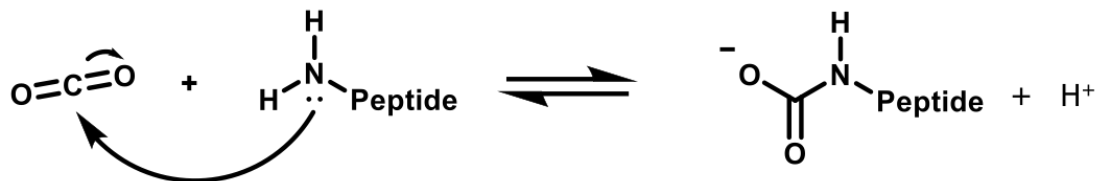
Figure 1.1| Mechanism of carbamate formation.

Carbamates are formed by the nucleophilic attack of a neutral amine on the carbon atom of carbon dioxide (Ewing et al., 1980; Hampe and Rudkevich, 2003). In proteins, this can occur at the N-terminal residue or on an epsilon-amine on the side chain of lysine residues. This results in a change of charge status, which influences protein structure and/or interactions with other molecules (Lorimer and Miziorko, 1980; Terrier and Douglas, 2010). Carbamylation is a labile modification that occurs within specific environments where the pKa of the amine group is below 9.5 (Chen et al., 1993; Jimenez-Morales et al., 2014). The pKa of lysine residues is typically between 9 and 13, which means that at physiological pH the amine is positively charged and consequently unable to form a carbamate (Abraham et al., 2009). However carbamates readily form at higher pH (Stadie and O'Brien, 1936). Thus it is thought that specific structural folds that harbour a lower pKa are required for carbamate formation (Cleland et al., 1998)

Le Chatelier's principle may be applied to carbamate formation. This principle states that when an equilibrium is subject to change, the equilibrium shifts in such a way as to counteract the change. This effectively nullifies the applied change. When applied to carbamate formation within a cellular context it is likely that the interaction between CO_2 and a neutral amine results in carbamate formation and a shift in the

equilibria to generate more neutral amines for further carbamate formation (Hackling and Garnett, 1985). Moreover, the sequestering of CO_2 by carbamate formation drives the dissociation of CO_2 from carbonic acid, which is utilised for further carbamate formation.

1.3. Examples of protein carbamylation

Carbamylation occurs on proteins found in all kingdoms of life (Table 1.1). There are a wide variety of physiological processes understood to be entirely dependent upon CO_2. Importantly, these proteins all demonstrate a physiologically relevant consequence of carbamylation i.e. the interaction of these proteins with CO_2 corresponds to a specific biological activity, rather than being an artefactual modification. Despite this, the list of proteins reported to undergo carbamylation is relatively short. It is anticipated that there are many more proteins that undergo carbamylation in a physiologically relevant manner but these have not yet been reported. This is due to a technical challenge concerning the identification of a labile modification. Here the carbamylation of two mammalian proteins is discussed.

Table 1.1| List of known protein carbamates.

Organism	Protein	Uniprot Accession	Site of Carbamylation	Reference
Homo sapiens	Haemoglobin	P68871	V1	(Lorimer, 1983)
Homo sapiens	Cx26	P29033	K125	(Meigh et al., 2013)
Spinacia oleracea	RuBisCO	P00875	K201	(Lorimer and Miziorko, 1980)
Klebsiella aerogenes	Urease	P18314	K217	(Yamaguchi and Hausinger, 1997)
Pseudomonas diminuta	Phosphotriesterase	G8DNV8	K169	(Benning et al., 2001)
Psuedomonas aeruginosa	β Lactamase	P14489	K70	(Golemi et al., 2001; Maveyraud et al., 2000)
Propionibacterium shermanii	Transcarboxylase	Q70AC7	K184	(Hall et al., 2004)
Geobacillus stearothermophilus	Alanine Racemase	P10724	K129	(Morollo et al., 1999)

1.3.1. Haemoglobin

Haemoglobin is well known for its role in oxygen transportation in red blood cells. Oxygen dissociation, and therefore tissue oxygenation, is encouraged by a phenomenon known as the Bohr effect. This is where an increased pCO_2 in the blood decreases the affinity of haemoglobin for oxygen, facilitating O_2 dissociation (Hsia, 1998). The deoxy-haemoglobin is then able to bind CO_2 to transport it from respiring tissues to the lungs, from where it is expelled from the body. The formation of N-terminal carbamates on deoxy-haemoglobin is responsible for up to 20% of CO_2 transport from tissues to the lungs (Lorimer, 1983; Vandegriff et al., 1991). CO_2 binds to neutral N-terminal amino groups of haemoglobin to form carbamate adducts with a preference for the β chains rather than α chains (Kilmartin et al., 1973; Matthew et al., 1977).

Dick et al. demonstrated that interference with N-terminal protonation perturbs carbamate adduct formation (Dick et al., 1999). This initially seems counterintuitive since it is the unprotonated amine group that is able to interact with CO_2 to form the adduct. Nonetheless Dick and colleagues show that perturbed carbamate adduct formation in these conditions is a true phenomenon because R141 is also deprotonated, removing the cationic species that serves to stabilise the anionic carbamate through electrostatic interactions (Dick et al., 1999). This is an important demonstration of carbamate stabilisation by the electrostatic interaction of a positively charged residue in close proximity to the labile carbamate.

1.3.2. Connexin 26

Another example of carbamate stabilisation is observed in Connexin 26 (Cx26). A recent paper demonstrated direct detection of CO_2 by Cx26, which is in contrast to the then commonly held belief that CO_2 detection occurred by proxy of pH changes

(Huckstepp et al., 2010a). Cx26 is a hemichannel that is sensitive to CO_2, with ATP release evoked upon activation of this gap junction in order to mediate downstream signalling events that regulate respiration (Huckstepp et al., 2010a). Cx26 is one of three connexins (Cx26, Cx30, and Cx32) that are sensitive to CO_2 (Meigh et al., 2013). During this investigation, the authors observed that a carbamylation motif, KVREI, is present in each of these hemichannels whereby carbamate formation at K125 is stabilised by formation of a salt bridge with R104. This carbamylation motif has been introduced to a CO_2-insensitive connexin, Cx31. The introduction of this motif showed CO_2-sensitive function in a manner analogous to WT Cx26. K125R or R104A mutation ablated the sensitivity of Cx26 to CO_2. Moreover, introduction of K125E to Cx26, which is analogous to carbamylated K125, resulted in a constitutively open hemichannel. It is clear from these genetic manipulations that carbamylation of K125 is required for appropriate activation of Cx26 in a CO_2-sensitive fashion. This has broad implications for vertebrate physiology, whereby it has been demonstrated that the affinity of Cx26 has evolved in a species-specific manner to suit the P CO_2 of the environment, highlighting the importance of respiratory regulation (de Wolf et al., 2017).

1.4. CO_2 in signalling pathways

Recent studies indicate that CO_2 acts effectively as a small signalling molecule. In particular, CO_2 alters the activity of many membrane transporters. This regulation can occur by direct interaction of CO_2 with the membrane protein or indirectly by signalling events typically downstream of CO_2-dependent changes to intracellular cAMP concentrations.

1.4.1. Direct CO_2 signalling

CO_2 binds to Cx26, a hemichannel, at K125 to form a carbamate bridge with R104 (Meigh et al., 2013). This interaction causes Cx26 to open, resulting in ATP efflux (Huckstepp et al., 2010b). This release of ATP has downstream effects that contribute

to the chemosensitive regulation of respiratory drive (Huckstepp et al., 2010a). In addition to Cx26 a K^+ influx channel, Kir, has also been reported to be responsive to direct binding of CO_2. However, a direct interaction between CO_2 and Kir has not yet been demonstrated (Huckstepp and Dale, 2011).

1.4.2. Indirect CO_2 signalling

Indirect regulation of membrane transporters by CO_2 is due to CO_2-dependent changes in cAMP levels (Turner et al., 2016). Na^+/HCO_3^- cotransporter (NBC) activity is upregulated in the context of elevated CO_2 levels (Adijanto et al., 2009), whilst Cl^- and fluid secretions by CFTR are reduced in similar conditions (Turner et al., 2016). This is in agreement with other research that observes CO_2-dependent decreases in cAMP production and corresponding cAMP-dependent signalling in kidney cells (Cook et al., 2012). However, there are also reported instances of CO_2-dependent increases in cAMP production and signalling (Lecuona et al., 2013; Townsend et al., 2009). Na^+/K^+ ATPase proteins are also negatively regulated in hypercapnic conditions (Briva et al., 2007). The role of CO_2 in the negative regulation of Na^+/K^+ ATPase activity is to upregulate Na^+/K^+ ATPase endocytosis (Vadasz et al., 2008). Thus, hypercapnia has differential effects of membrane transporter activity that is cell type and tissue context dependent. A challenge going forwards is to define the exact mechanism of action of CO_2 in these signalling pathways. The binding site of CO_2 is known for Cx26 and this has been informative to deepen the understanding of the regulation of this protein. Such clarity is desired for the other signalling processes described.

1.4.3. NFκB Signalling

The NFκB family of transcription factors belong to one of two distinct signalling pathways, canonical and non-canonical. Release of the active transcription factor is essential in both pathways, and the mechanism by which it is released categorises the type of NFκB pathway.

Canonical NFκB signalling requires the proteasomal degradation of IκB to release NFκB, whilst non-canonical NFκB signalling requires the proteolytic processing of precursors. Typically, p100 and p105 are cleaved to p52 and p50, respectively, which form a heterodimer to achieve transcriptional regulation.

1.4.3.1. *Canonical NFκB signalling*

The key irreversible step in canonical NFκB signalling is the release of the cytoplasmic inhibitor, IκB, via proteolysis. IκB degradation releases NFκB, allowing for nuclear translocation and subsequent association with DNA to initiate transcription of target genes. One of these target genes is IκB, which associates with NFκB to perform nuclear export of the transcription factor (Brown et al., 1993; Karin and Ben-Neriah, 2000). Therefore, the activation and termination of NFκB mediated gene expression is tightly regulated by IκB (Beg et al., 1993; Sun et al., 1993).

Initial experiments demonstrating dissociation of IκB as an important activation step in NFκB signalling were performed using detergent (Baeuerle and Baltimore, 1988). Furthermore, it was revealed that phosphorylation of IκB was essential for its degradation and that inhibiting IκB degradation prevented NFκB activation. This group also demonstrated that phosphorylation alone was not sufficient for NFκB activation, suggesting an additional regulatory factor is involved (Henkel et al., 1993). This additional layer of regulation was demonstrated to be ubiquitination and subsequent proteasomal degradation of phosphorylated IκB (Alkalay et al., 1995; Chen et al., 1995).

In the canonical NFκB pathway elevated CO_2 has been shown to induce reversible IKK nuclear translocation (Cummins et al., 2010). IKK phosphorylates IκB, thus priming it for ubiquitination and proteasomal degradation. The nuclear translocation of IKK prevents phosphorylation of IκB. This in turn prevents degradation of IκB so that NFκB

remains sequestered in the cytoplasm. It is unclear where exactly CO_2 modulates the activity of the signalling cascade, since there are multiple upstream steps that could be influenced. This suppression of NFκB signalling results in innate immune suppression, which is also observed in rats that are still able to perform renal buffering, suggesting the effect is CO_2 mediated and independent of pH (Nichol et al., 2009). It is thought that CO_2-mediated immune suppression may be beneficial to the overall health of an individual as a method of tolerating metabolic stress (Amato et al., 1998; Hanly et al., 2006; Laffey et al., 2004).

1.4.3.2. *Non-canonical NFκB signalling*

In the non-canonical NFκB signalling pathway ubiquitination and proteasomal degradation enables the generation of the active NFκB subunit, p50, from its precursor, p105 (Palombella et al., 1994). Sequence homology identified a conserved N-terminal sequence containing two serine residues, at positions 32 and 36, that are essential for phosphorylation and subsequent ubiquitin-mediated IκB degradation by the proteasome (Brown et al., 1995; Chen et al., 1995; Yaron et al., 1997). The importance of this conserved sequence was highlighted by comparing the half-life of IκB in resting cells and activated cells. In the former the half-life is approximately 140 minutes, whilst in activated cells it is approximately 1.5 minutes (Henkel et al., 1993).

An SCF E3 ligase is responsible for the ubiquitination of phosphorylated IκB, p100 and p105 for their subsequent interaction with the proteasome (Fong and Sun, 2002; Heissmeyer et al., 2001; Orian et al., 2000; Wu and Ghosh, 1999). It achieves this by bringing the substrate lysine of IκB into closer proximity to the E2~ubiquitin complex, permitting more efficient ubiquitin transfer (Wu et al., 2003). The SCF E3 ligase recognises phosphorylated proteins through its beta-TrCP subunit (Yaron et al., 1998). Its ability to differentiate between various substrate phosphoproteins is due to the protein recognition subunit, F box protein (FBP), which has a protein recognition domain at its C-terminus (Cardozo and Pagano, 2004; Deshaies, 1999).

Members of the non-canonical NFκB signalling pathway have been reported to be sensitive to CO_2 (Oliver et al., 2012). This effect has also been observed in downstream genes of Relish, an NFκB orthologue in *D. melanogaster* (Helenius et al., 2009). A recent paper recorded the first identification of a conserved 20 amino acid CO_2 responsive domain (CORD) located at the C-terminus of RelB (Keogh et al., 2017). RelB is subject to multiple PTMs (Hailfinger et al., 2009; Marienfeld et al., 2001; Neumann et al., 2011). After being subject to hypercapnic conditions RelB is cleaved at the CORD (Keogh et al., 2017). The CORD is situated within the transactivation domain of RelB, which explains the reduced NFκB mediated gene expression observed in hypercapnic conditions (Perkins, 2007). It was also shown that p100 nuclear translocation occurs, and this is thought to be important for the NFκB-dependent response to CO_2 (Keogh et al., 2017). One explanation for this may be due to the prerequisite of p100 processing to p52 for normal non-canonical NFκB signalling activation. The intact p100 subunit may prevent DNA binding through the Rel homology domain and consequently attenuate non-canonical NFκB signalling. In addition to this the polyubiquitination of RelB augments transcriptional activity. This occurs despite K48R K63R double mutants of ubiquitin (Leidner et al., 2008). This suggests that ubiquitin is linked through isopeptide bonds formed at alternative lysine residues to K48 and K63.

It was recently identified that heat shock factor 1 (HSF1), a heat shock protein, is upregulated in hypercapnia. This is associated with decreased expression of proinflammatory cytokines (Lu et al., 2018). HSF1 has previously been implicated as a NFκB inhibitor, which suggests the mechanism for hypercapnic immune suppression is through increased expression of HSF1 (Lu et al., 2018; Song et al., 2008).

1.4.3.3. D. melanogaster development

Embryonic development and egg laying are developmental processes that are perturbed by hypercapnic conditions. This is independent of the CO_2 sensitive neurones, Gr63a (Helenius et al., 2009). RNAi knockdown of Zfh2 partially restored the effects of elevated CO_2 on egg hatching (Helenius et al., 2016a).

1.5. CO_2 in pathology

1.5.1. Perturbed fluid reabsorption in pulmonary disease

Patients with acute respiratory distress syndrome (ARDS) or COPD present with hypercapnia. Fluid reabsorption at the alveolar epithelium is critical to maintaining optimal gas exchange in the lungs. This is achieved by the active transport of fluid into the cell by the Na^+/K^+ ATPase (Matthay et al., 2002; Sznajder, 2001; Vadasz et al., 2007). Hypercapnia decreases Na^+/K^+ ATPase activity, which impairs alveolar fluid reabsorption and leads to alveolar epithelial dysfunction (Briva et al., 2007; Vadasz et al., 2008). This is also observed in *Drosophila* (Helenius et al., 2009). Decreased Na^+/K^+ ATPase is achieved through JNK-dependent endocytosis of the Na^+/K^+ ATPase. Here, AMPK and PKC-zeta are activated which causes activation of JNK through its phosphorylation at S129 (Vadasz et al., 2012). Endocytosis of this pump, and the resulting alveolar epithelial dysfunction, worsens prognosis in patients with COPD and ARDS.

1.5.2. Muscle atrophy in pulmonary disease

Muscle atrophy is recognised as a major contributor to worse clinical outcomes in patients with pulmonary disease (Celli et al., 2004) and recovery of muscle mass in COPD patients has proven to be beneficial to pulmonary rehabilitation (Puhan et al., 2011). Recent research has demonstrated that hypercapnia stimulates skeletal muscle degradation via the ubiquitin proteasomal degradation pathway (Jaitovich et al.,

2015). Here, $AMPK_{\alpha2}$ is readily phosphorylated in the presence of elevated CO_2 levels. This causes an increase in FoxO3a activation which in turn upregulates expression of muscle-specific ubiquitin-E3 ligases muscle RING finger 1 (MuRF1). The upregulation of MuRF1 in muscle atrophy is consistent with other reports despite different upstream signalling events occurring (Glass, 2005). The results obtained by Jaitovich and colleagues showed that the hypercapnia-induced muscle atrophy was independent of pH change and therefore this effect must be due to carbamylation. The substrate for carbamylation has not been identified.

1.5.3. Hypercapnia mediates immune suppression

Hypercapnia induces expression of metabolic and decreases expression of immune genes in *Drosophila* (Helenius et al., 2009). This was shown to be independent of a neuronal CO_2 sensing pathway, suggesting a role for a cell autonomous CO_2 sensing pathway. The identified genes repressed in hypercapnia are under regulatory control of the NFκB transcription factor. Similarly, studies in mammalian alveolar macrophages have implicated NFκB in a CO_2–responsive signalling pathway whereby increased levels of CO_2 suppress expression of proinflammatory cytokines (Wang et al., 2010). Importantly, both of these aforementioned studies demonstrated the effect of hypercapnia on immune suppression (1) was independent of acidosis, (2) increased mortality from specific bacterial infection, and (3) occurred independently of IκB proteolysis in the NFκB pathway. These results suggest an evolutionary conserved mechanism of CO_2 signalling that regulates immune and inflammatory pathways with physiological consequences.

A recent RNAi screen identified Zfh2 as a mediator of hypercapnic immune suppression in *D. melanogaster* (Helenius et al., 2016a). Zfh2 is expressed in adipose tissue, which is the major immune organ of *Drosophila*. Knockdown of Zfh2 in ex-vivo cultured fat bodies expressed 2-fold more diptericin compared to control in buffered hypercapnic conditions. This corresponds to improved survival of *S. aureus* infection.

Zfh2 has mammalian homologs, ZFHX3 and ZFHX4. It is not yet understood whether these transcription factors also mediate hypercapnic immune suppression in mammals but if this were confirmed it would suggest an evolutionary conserved pathway through which CO_2 mediates immune suppression. The authors of this investigation are quick to point out that there is more to be understood about this process. In particular, it is likely that Zfh2 is the effector and that the CO_2 sensor is yet to be identified (Helenius et al., 2016a).

Several compounds have recently been identified that improve the expression of antimicrobial peptides during hypercapnia (Helenius et al., 2016b). Of these, evoxine, a furoquinolone alkaloid, increased the expression of the pro-inflammatory cytokines IL-6 and CCL2 in mammalian alveolar macrophages during hypercapnia. This is the first demonstration of using a small pharmacological compound to reverse the effects of hypercapnia, which provides the platform upon which further research can aim to therapeutically target hypercapnic pathologies. Of particular importance will be structural studies that elucidate the precise interaction between these small molecules and their targets. This will inform future studies aiming to generate pharmacological agents with which to treat pathologies actively enhanced by elevated CO_2 levels.

1.6. Thesis outline

The biological question underpinning this work is how cells sense and respond to changes in CO_2 levels. CO_2 is a product of aerobic respiration and could therefore act as a signalling molecule to contribute to the metabolic status of the cell. A greater understanding of this biological phenomenon will broaden understanding of fundamental biological processes linking cellular metabolism and homeostasis. Elevated CO_2 levels are observed in patients with pulmonary disease and this hypercapnia has been reported to worsen prognosis. Therefore, this work will also

contribute to a greater understanding of the pathophysiology of these diseases which, in turn, will lead to the development of therapies to treat these diseases.

CO_2 has previously been demonstrated a) to bind directly to proteins to form carbamates b) to be involved in cellular signalling processes c) to both directly and indirectly regulate protein activity and d) to contribute to pathological states. A recent proteomics using *A. thaliana* leaf lysate investigation suggests ubiquitin is susceptible to carbamylation (Linthwaite, 2016). In this screen ubiquitin was identified as a high confidence candidate, with a similarly low probability of error score as RuBisCO, a bona fide target of CO_2-dependent carbamylation. Despite this, carbamate formation on ubiquitin was not validated.

Ubiquitin is a small (~8 kDa) evolutionary conserved protein with broad signalling functions (Chen, 2005; Finley and Chau, 1991). Ubiquitin is conjugated to substrate proteins through a series of reactions catalysed by enzymes from the 3 classes of ubiquitin ligases. The activating E1 ligase forms a thiol ester with the carboxyl group of ubiquitin G76. The conjugating E2 ligase forms a thiolester with G76. The E3 ligase transfers ubiquitin from the E2 ligase to the substrate, forming an isopeptide bond between the substrate lysine Nε-amine group and G76 of ubiquitin (Pickart, 2001). A polyubiquitin chain forms when further ubiquitin molecules are conjugated. The diverse array of ubiquitin signalling is conferred through the type and mode of ubiquitin cross-linking. PTMs occurring on ubiquitin itself regulate its ability to cross-link (Matsuda, 2016). CO_2-dependent carbamylation and ubiquitin cross-linking both occur on lysine residues, suggesting a physiologically relevant role for ubiquitin carbamylation.

Altogether, the hypothesis of this work is that CO_2 binds directly to ubiquitin with physiologically relevant consequences. To investigate this hypothesis a mass

spectrometry approach is taken to investigate CO_2-dependent carbamate formation on ubiquitin. Upon confirmation of two sites of carbamylation, a functional assay is performed to investigate the consequence of carbamate formation.

2. Methods

2.1. *E. coli* strains

Table 2| *E. coli* strains and genotypes used for expression of recombinant proteins.

Strain	Genotype
BL21 (DE3)	F⁻ *ompT hsdS*$_B$ (r$_B$⁻ m$_B$⁻) *gal dcm* (DE3)
Rosetta (DE3) pLysS	F⁻ *ompT hsdS*$_B$(r$_B$⁻ m$_B$⁻) *gal dcm* (DE3) pLysSRARE (Cam^R)
Rosetta 2 (DE3) pLysS	F⁻ *ompT hsdS*$_B$(r$_B$⁻ m$_B$⁻) *gal dcm* (DE3) pLysSRARE2 (Cam^R)

2.2. Protein expression and purification

2.2.1. pET 28 mE1

BL21 (DE3) were transformed with *pET28 mE1* (a gift from Jorge Eduardo Azevedo (Addgene plasmid #32534)) and protein expression was induced by addition of 0.5 mM IPTG at an OD$_{600}$ 0.6 for 20 hours at 16°C (Carvalho et al., 2012). Cells were harvested at 4000 g and subjected to a freeze-thaw cycle before being resuspended in E1 Lysis buffer (50 mM Tris-HCl pH 8.0, 150 mM NaCl 0.1% (w/v), Triton X-100, 1 mM EDTA-NaOH pH 8.0, 1 mM DTT, 0.1 mg/mL phenylmethylsulfonyl fluoride, 1:500 (v/v) Sigma mammalian protease inhibitor mixture) and lysed by sonication. The soluble fraction was obtained after centrifugation at 21,000 g and incubated with 0.5 mL Ni^{2+} NTA resin per 1 L pellet for 2 hours at 4°C with end to end agitation. The resin was washed with 15 BV wash buffer (50 mM sodium phosphate pH 8.0, 150 mM NaCl) and eluted with 3 x 1 BV elution buffer (wash buffer, 100 mM imidazole). The eluted fractions were resolved on SDS-PAGE and fractions containing mE1 were pooled, concentrated and buffer exchanged into AEC buffer (10 mM Tris-HCl pH 8.0, 0.1 mM

EDTA-NaOH pH 8.0, 1 mM DTT). This was loaded onto Bio-Scale Mini Macro-Prep High Q Cartridge (Bio-Rad) at a flow rate of 0.5 ml/min. and eluted with a linear gradient of 0 - 0.5 M NaCl in AEC elution buffer (AEC buffer, 0.5 M NaCl). Following buffer exchange to SEC Buffer (20 mM Tris HCl pH 8.0, 100 mM NaCl, 1 mM EDTA-NaOH pH 8.0, 1 mM DTT) mE1 was loaded onto Superose 12 column HR 10/30 (GE Healthcare) with flow rate of 0.5 mL/min and fractions were resolved by SDS-PAGE. Fractions containing mE1 were pooled, concentrated, and stored at -80°C.

2.2.2. pGEX-4T E2-25K

Rosetta (DE3) pLysS cells were transformed with *pGEX-4T E2-25K* (a gift from Titia Sixma (Addgene plasmid #63572)) and grown to an OD$_{600}$ 0.7 at 37°C. GST-E2-25K expression was induced with 0.5 mM IPTG for 20 hours at 16°C (Pichler et al., 2005). Cells were harvested at 4000 g and subjected to a freeze-thaw cycle before being resuspended in E2 Lysis buffer (50 mM Tris-HCl pH 7.6, 1 mM EDTA, 2 mM DTT, 1 mM PMSF) and lysed by sonication. The soluble fraction was obtained following centrifugation at 21,000 g and passed over 0.8 mL SuperGlu resin per 1 L pellet at a flow rate of 0.5 mL/min. The resin was then washed with 10 BV 1x PBS before GST-E2-25K (herein referred to as E2-25K) was eluted with 1 BV 1x PBS, 10 mM reduced glutathione and dialysed for 16 hours into GF buffer (20 mM Tris-HCl pH 8.0, 300 mM NaCl, 1 mM DTT, 1 mM EDTA). E2-25K was then loaded onto a Superdex 75 column at a flow rate of 1 mL/min. Fractions were resolved by SDS-PAGE and those containing E2-25K were pooled, concentrated, and stored at -80°C.

2.2.3. Ubiquitin (*Homo sapiens*)

BL21 (DE3) cells containing *pET28 UBC* (a gift from Rachel Klevit (Addgene plasmid #12647)) were grown to an OD$_{600}$ 0.6. Ubiquitin expression was induced with 0.5 mM IPTG for 16 hours at 16°C (Brzovic et al., 2006). Cells were harvested at 4000 g and lysed by sonication in 50 mM Tris-HCl pH 8.0, 150 mM NaCl, 0.1% (w/v) Triton X-100, 1 mM EDTA-NaOH pH 8.0, 1 mM DTT, Protease inhibitor cocktail (Thermo Scientific). Soluble protein was separated from cell debris by centrifugation at 21,000 g and

incubated with 1 mL Ni^{2+}-NTA resin (50% slurry) for 2 hours with end to end shaking. Weakly bound protein was washed with 10 BV 50 mM Tris-HCl pH 8.0, 150 mM NaCl, 10 mM Imidazole. Bound protein was eluted across a range of 50 mM – 250 mM imidazole. Each protein fraction was stored at $-80^{o}C$ in elution buffer with 20% glycerol.

2.2.4. <u>Ubiquitin (Arabadopsis thaliana)</u>

Rosetta 2 (DE3) pLysS cells containing *pET30a UBQ11* (a gift from Ari Sadanandom) were grown to an OD_{600} 0.7, at which point Ubiquitin expression was induced with 1 mM IPTG for 4 hours at $37^{o}C$ (Pangestuti, 2009). Cells were harvested at 4000 g and lysed in 50 mM Tris-HCl pH 8.0, 150 mM NaCl, 1 mM EDTA-NaOH pH 8.0, protease inhibitor cocktail (Sigma). Soluble protein was separated from cell debris by centrifugation at 21,000 g before incubation with 2 mL Ni^{2+}-NTA resin (50% slurry) for 1.5 hours with end to end shaking. Weakly bound protein was washed with 10 BV 50 mM Tris-HCl pH 8.0, 150 mM NaCl, 10 mM Imidazole. Bound protein was eluted across a range of 50 mM – 250 mM imidazole. Each protein fraction was stored at $-80^{o}C$ in elution buffer with 20% glycerol.

2.3. CO_2 trapping experiment

0.5 mg purified recombinant protein was dialysed into 50 mM Phosphate Buffer pH 7.4. The trapping reaction mixture was supplemented with 20 mM $NaHCO_3$ and the trapping reaction was initiated by addition of 10x molar excess of TEO. The total volume for the trapping reaction was 4 mL at t=0 and titration of 1 M NaOH ensured that the pH was maintained at 7.4 for 1 hour before terminating the reaction by dialysing into dH_2O.

2.4. Physical Chemistry

2.4.1. FASP Trypsin Digest

Following dialysis the insoluble protein was obtained by centrifugation at 5000 g for 10 minutes. The protein aggregate was resuspended in 1% SDS and trypsinolysis was performed using the FASP trypsin digest kit according to the manufacturer's protocol (Wisniewski et al., 2009).

2.4.2. Sample concentration using ZipTip

TFA was added to samples at a final concentration 0.01 % (v/v). Washing was performed with 100 % acetonitrile and then equilibrated with 0.1 % TFA. 30 μL sample was immobilised and washed with 0.1 % (v/v) TFA. Finally, peptides were eluted in 0.1 % TFA 50 % acetonitrile (v/v).

2.4.3. Sample fractionation using StageTip

Sample fractionation was performed using a C18 StageTip according to manufacturer's protocol (Rappsilber et al., 2007). Peptides were fractionated using a 50 – 500 mM ammonium acetate gradient.

2.4.4. MALDI-TOF MS

0.3 μg peptide samples were mixed with α-CHCA, 50 % CAN, 0.05 % TFA at a ratio 1:1 and applied to the MALDI plate. Following 20 min incubation at room temperature the plate was placed in the ion source. Data collection was performed using 4800 plus TOF/TOF Analyzer (SCIEX) utilising 100 pulse shots with variable laser intensity.

2.4.5. LC-MS/MS

0.3 μg samples were resuspended in 2 % ACN, 0.1 % formic acid and injected at a flow rate 0.1 mL/min over a 2 hour gradient from 2 – 80 % ACN, 0.1 % formic acid. Peptides eluted from the acetonitrile gradient were resolved using TripleTOF 6600 Quadrupole time of flight (QTOF; SCIEX) in data dependent acquisition (DDA) mode implementing top 30 precursor ion selection over 10 ms acquisition time. Selected peptide fragmentation was achieved by CID.

2.4.6. Data Analysis

The LC-MS/MS data was analysed using the GPM database X!Tandem and MaxQuant. Carbamidomethyl cysteine was searched for as a fixed variable, whilst carboxyethyl (72.0211 Da) and ethyl (28.0313 Da) transfer were searched for as variable modifications. Parent ion mass error was set to +/- 20 ppm and reverse peptides were enabled. The searches were performed against Human (SwissProt) and *Arabadopsis thaliana* (UniProt) databases.

2.5. Ubiquitin cross-linking assay

The cross-linking assay contained 0.75 μM mE1, 20 μM E2-25K, and 1.2 μM Ubiquitin. Reactions were performed in 250 mM Tris-HCl pH 8.0, 25 mM $MgCl_2$, 2.5 mM ATP, 1 mM DTT, 50 mM Creatine Phosphate (Roche, 0621714001), 3 U/mL inorganic pyrophospatase (Sigma, I1643), and 3 U/mL Creatine phosphokinase (Sigma, C3755). 35 mM NaCl and 35 mM $NaHCO_3$ pH 8.0 were added to the appropriate assays. Reactions were carried out in a final volume of 50 μL at $37^{o}C$ for 15 minutes, terminated by the addition of 1 mM EDTA and reducing the temperature to $4^{o}C$ for 15 minutes. Samples were resolved by SDS-PAGE following incubation with non-reducing Laemmli buffer for 20 minutes.

3. Results

When CO_2 interacts with uncharged $N\epsilon$-amine groups of lysine residues a carbamate is generated, which changes the electrostatic properties of the protein (Lorimer and Miziorko, 1980). Ubiquitin is a small (~8 kDa) protein involved in a wide array of signalling process. The diverse range of signalling pathways influenced by ubiquitin is only possible because of the many different combinations of ubiquitin crosslinking to form various polyubiquitin chains (Zinngrebe et al., 2014). Polyubiquitin chain synthesis requires isopeptide bond formation between $N\epsilon$-amine groups of lysine residues and the C-terminal glycine of the next ubiquitin. PTMs, such as acetylation and phosphorylation, are known to impact on the rate of polyubiquitin chain formation (Ohtake et al., 2015; Wauer et al., 2015). Therefore, the overall hypothesis of this work is that CO_2 binds directly with $N\epsilon$-lysine of ubiquitin to confer a biological signal modulating the rate of polyubiquitin chain formation. The initial aims were to identify sites of CO_2-dependent carbamylation of ubiquitin and consequently to define a change in function associated with the PTM. Here, MALDI-TOF (hereafter referred to simply as MALDI) and LC-MS investigations prove that K33 and K48 of ubiquitin are sites of CO_2-dependent carbamylation. This is followed by an *in vitro* cross-linking assay that suggests carbamate formation reduces the rate of ubiquitin discharge from its E2 ligase, which provides a mechanism to support the overall hypothesis.

3.1. Recombinant protein expression

Recombinant *A. thaliana* and *H. sapiens* His$_6$-ubiquitin were expressed in Rosetta 2 pLysS and BL21 (DE3) cells, respectively, and purified by immobilized metal affinity chromatography (IMAC) (Figure 3.1.A, B, respectively). These proteins have high sequence similarity (Figure 3.1.G) and were deemed to be greater than 95 % pure by densitometry (data not shown). For both ubiquitin samples fractions 1 – 5 were pooled and concentrated for use in MS investigations and in vitro crosslinking assays. His$_6$-mE1 was expressed in BL21 (DE3) and purified by IMAC (Figure 3.1.C). The three elution fractions were pooled, concentrated and purified by AEC (Figure 3.1.C). Fractions corresponding to Fig 1.C lanes 6 and 7 were further purified by SEC (Figure 3.1.D). These fractions were determined to be > 98 % pure by densitometry

and were pooled and concentrated for us in *in vitro* crosslinking assays. GST-E2-25K was expressed in Rosetta (DE3) pLysS and purified by affinity chromatography (Figure 3.1.E). GST-E2-25K was further purified by SEC (Figure 3.1.F), with fractions corresponding to lanes 2-11 pooled and concentrated for use in *in vitro* crosslinking assays.
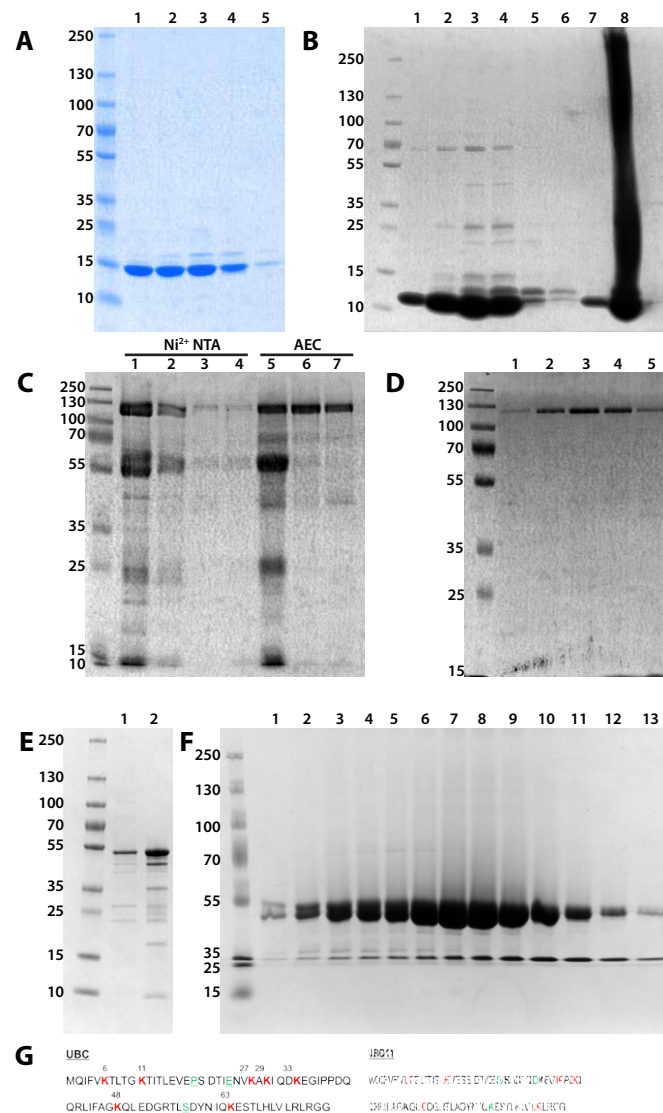
Figure 3.1| Recombinant protein expression resolved by SDS-PAGE. A) Ni^{2+} NTA purification of *A. thaliana* ubiquitin. Lanes 1 – 5: 50 – 250 mM imidazole elutions, respectively. B) Ni^{2+} NTA purification of *H. sapiens* ubiquitin. Lanes 1 – 5: 50 – 250 mM imidazole elutions, respectively. Lanes 6 – 8: 1 M imidazole fraction, pooled and concentrated fractions 1 – 5, and insoluble fraction, respectively. C) mE1 purification. Lanes 1 – 4: final wash and 3x 100 mM elutions. Lanes 5 – 7: AEC fractions. D) Lanes 1 – 5: mE1 SEC fractions. E) GST-E2-25K purification. Lane 1-2: final wash fraction and 10 mM glutathione elution, respectively. F) GST-E2-25K SEC fractions. Lanes 2 – 12 (inclusive) were pooled for future use.

G) sequences of *A. thaliana* and *H. sapiens* ubiquitin. Lysine residues are highlighted in bold red typeface and their position is annotated. Differing residues are highlighted in green underlined typeface.

3.2. Confirmation of Trapped Carbamates using TEO by detection with MALDI-TOF

Carbamates are labile and thus their identification by MS remains a technical challenge. Recently, a method to trap carbamates with an alkylating reagent, triethyloxonium tetrafluoroborate (TEO), has been developed in which carboxylic acid groups are ethylated, introducing a modification with a mass of 28.0303 Da (Linthwaite, 2016). A trapped carbamate is recognised as a carboxyethyl modification, which has a mass of 72.0211 Da. This modification is stable and can be detected by MS after the protein has been digested by trypsin. MALDI is a quick, low cost form of MS that rapidly identifies peptides. Since the mass of a peptide modified by the reaction with TEO can be calculated, the hypothesis of this investigation is that carboxyethylated peptides can be detected by MALDI.

The trapping experiment was performed using recombinant *A. thaliana* and *H. sapiens* Ubiquitin in solution with 20 mM NaHCO$_3$ pH 7.4 and a molar excess of TEO. This was followed by tryptic digest and the resulting peptides were analysed by MALDI. Given that MALDI measures peptides by mass, a key question is how can a distinction be made between a carboxyethylated peptide and a random isobaric peptide? The solution to this problem can be found by searching for an ethylation series corresponding to the peptide of interest. An ethylation series is generated when a protein is differentially ethylated during the reaction with TEO. Following trypsinolysis, this gives rise to a number of detected peptides increasing by 28.0303 Da (i.e. the mass of an ethylation). Therefore, ethylation series are a positive control to demonstrate the reaction with TEO has taken place on the peptide of interest. If the peptide of interest has a 72.0211 Da modification within an ethylation series, it can be deduced that this is an ethylated carbamate. An ethylation series was obtained for

two peptides of ubiquitin, [43]LIFAGKQLEDGR[54] and [30]IQDKEGIPPDQQR[42] (Table 3.1 and 3.2, respectively).

Table 3.1| Ethylation series of tryptic digest peptide corresponding to carboxyethylation of K48 of ubiquitin. Only peptides with K48 miscleavage are considered. The predicted mass is accurate ± 0.5 Da. Et = ethylation, Ce = carboxyethylation.

[43]LIFAGKQLEDGR[54]		
Predicted mass	Detected Peptide Mass	Modification
1346.74272	-	-
1374.77402	1374.753174	Et
1402.80532	1402.781738	2x Et
1418.76382	1418.723389	Ce
1446.79512	1446.714722	Ce, Et
1474.82642	-	Ce, 2x Et

It was hypothesised that carboxyethylated peptides could be identified by MALDI-TOF. It is possible to infer the existence of such peptides by delineating the ethylation series of the peptide. Using this approach, a 1418.723 Da peptide was confirmed as the carboxyethyl peptide corresponding to [43]LIFAGK(Ce)QLEDGR[54] (table 3.1). A second carboxyethylated peptide was detected as part of an ethylation series with a 1595.799 Da mass that corresponds to [30]IQDK(Ce)EGIPPDQQR[42] (table 3.2). These ethylation series are a strong indicator that the carboxyethyl peptides were derived downstream of the reaction with TEO and it can thus be accepted that carboxyethylated peptides can be detected by MALDI.

Table 3.2| Ethylation series of tryptic digest peptide corresponding to carboxyethylation of K33 of ubiquitin. The predicted mass is accurate ± 0.5 Da. Et = ethylation, Ce = carboxyethylation.

[30]IQDKEGIPPDQQR[42]		
Predicted mass	Detected Peptide Mass	Modification
1523.78129	1523.763428	-
1551.81259	1551.792236	Et
1579.84389	1579.82312	2x Et
1595.80239	1595.79895	Ce
1623.83369	1623.817383	Ce, Et
1651.86499	-	Ce, 2x Et

Other peptides with a mass corresponding to carboxyethyl modification were also identified (Table 3.3). However, an ethylation series could not be derived for these peptides. Therefore, it is not possible to confirm the presence of the carboxyethyl modification as a direct result of the trapping reaction with TEO.

Table 3.3| Peptides of interest detected by MALDI without a corresponding ethylation series. The predicted mass is accurate ± 0.5 Da. Et = ethylation, Ce = carboxyethylation.

Sequence	Predicted Peptide Mass	Detected Peptide Mass	Modification
[12]TITLEVEPSDTIENVKAK[29]	2059.08052	2059.023193	Ce
[28]AKIQDKEGIPPDQQR[42]	1822.96578	1822.954	Ce, Et
[28]AKIQDKEGIPPDQQR[42]	1850.99706	1850.976	Ce, 2x Et
[55]TLSDYNIQKESTLHLVLR[72]	2225.20678	2225.098145	Ce, Et

The aim of this investigation was to identify peptides with the carboxyethyl modification indicative of a trapped carbamate. Identification of a peptide was achieved by comparing predictive mass with the mass of peptides detected by MALDI. If a suspected carboxyethylated peptide is detected and found to have a corresponding ethylation series it can be concluded that a carboxyethyl modification was likely derived from the trapping reaction with TEO. However, if an ethylation series does not exist the most likely explanation is that an isobaric peptide was actually detected. In this investigation two peptides, corresponding to carboxyethylated L43-R54 and I30-R42, were identified concurrently with respective ethylation series. This confirms the initial hypothesis and therefore, the aim of this investigation has been achieved.

3.3. Confirmation of Ubiquitin carboxyethyl modification at K33 and K48 by LC-MS

In the previous investigation, it was demonstrated that carboxyethylated peptides could be detected and confirmed by MALDI and an ethylation series, respectively (Chapter 3.1). This confirms the trapping reaction with TEO occurred but does not

provide accurate information regarding the modified residue. Consequently, this investigation aims to identify the specific site of modification in the peptide sequence. It is known that carbamates are formed at uncharged Nε-amino groups. Therefore, the hypothesis of this investigation is that carboxyethyl modifications occur at lysine residues. The trapping reaction was performed with both *A. thaliana* and human recombinant ubiquitin. Following tryptic digest, peptides were resolved by LC-MS/MS and the MS2 data was compared with the corresponding Uniprot proteome databases using X!Tandem. Using this approach it was confirmed that K33 and K48 are sites of carboxyethyl modification.

Table 3.4| Ubiquitin peptides identified with carboxyethyl modification. Ce = carboxyethylation, Et = Ethylation.

Organism	Peptide	Modifications	Identified m+h by LC-MS/MS	Log(e)	False Positive
A. thaliana	^{7}TLTGKTKVLEVESSDTIDNVK^{27}	K11Ce, E18Et	2377.27080	-3.4	√
	^{7}TLTGKTKVLEVESSDTIDNVK^{27}	K13Ce	2349.23950	-4.4	√
	^{28}AKIQDKEGIPPDQQR^{42}	K29Ce	1794.93448	-6.5	√
	^{28}AKIQDKEGIPPDQQR^{42}	K29Ce, D32Et	1822.96578	-4.9	√
	^{28}AKIQDKEGIPPDQQR^{42}	K29Ce, D39Et	1794.960	-4.2	√
	^{28}AKIQDKEGIPPDQQR^{42}	K29Ce, D32Et, E34Et	1850.99706	-3.7	√
	^{30}IQDKEGIPPDQQR^{42}	K33Ce	1595.80237	-5.8	
	^{28}AKIQDKEGIPPDQQR^{42}	K33Ce	1794.93448	-4.7	√
	^{30}IQDKEGIPPDQQR^{42}	K33Ce, E34Et	1623.83367	-5.6	
	^{43}LIFAGKQLEDGR^{54}	K48Ce	1418.76378	-3.3	
	^{43}LIFAGKQLEDGR^{54}	K48Ce, E51Et	1446.79508	-4.0	
H. sapiens	^{28}AKIQDKEGIPPDQQR^{42}	K29Ce, D32Et	1822.96575	-5.5	√
	^{28}AKIQDKEGIPPDQQR^{42}	K29Ce, D32Et, E34Et	1850.99705	-3.1	√
	^{30}IQDKEGIPPDQQR^{42}	K33Ce	1595.80237	-4.7	
	^{30}IQDKEGIPPDQQR^{42}	K33Ce, E34Et	1623.83367	-4.5	
	^{43}LIFAGKQLEDGR^{54}	K48Ce	1418.76378	-3.3	
	^{43}LIFAGKQLEDGR^{54}	K48Ce, E51Et	1446.79510	-4.5	
	^{43}LIFAGKQLEDGR^{54}	K48Ce, E51Et	1432.77945	-5.8	

The hypothesis of this investigation is that carboxyethyl modifications occur at Lysine residues in the ubiquitin sequence. Using LC-MS/MS paired with X!Tandem protein identification software enabled the identification of carboxyethyl (72. 0211 Da) and ethyl (28.0313 Da) modifications to specific residues along peptide sequences. This approach resulted in 11 and 7 carboxyethyl modified peptides for *A. thaliana* and human ubiquitin, respectively (Table 3.4). Not all the carboxyethyl modifications recorded are true positives. This is demonstrated in figure 3.1, where manual inspection of the fragmentation pattern clearly demonstrates there are no matched peptides for fragments that include the lysine reported to be carboxyethyl modified. This indicates a weak correlation between the detected peptide and the database entry. In addition to this the peptide is matched with the gene product of *A. thaliana* UBQ12, which has a lysine residue at position 13 of its sequence (figure 3.1). This is

clearly incorrect because recombinant ubiquitin was generated from *A. thaliana* UBQ11 or human UBC gene, which have an isoleucine residue at this position. These are examples of how the software can assign the detected mass to a peptide in the database to generate a false positive. Therefore it is imperative to manually inspect each MS2 data in order to validate the assigned peptide is a true positive. In addition to matched fragments, the log(e) score, which is the likelihood of the peptide being matched with a random peptide, is a good indicator of the accurate assignment of a detected peptide to a peptide in the database. The lower the log(e) score the higher the confidence in the assignment. This approach was used to assess the results generated by X!Tandem peptide assignment (table 3.4).

a) ^{12}C K11(Ce) I13K K13(miscleavage) E18(Et)

log(e)	m+h	sequence
-3.4	2377.27080	iflk^7 TLTGKTKVLEVESSDTIDNVK^{27}akiq

mods: K11+Carboxyethyl, E18+Dimethyl

T L T G K T K V L E V E S S D T I D N V K

bond	+1y
T1	2276.223
L2	2163.139
T3	2062.091
G4	2005.070
K5	1804.954
T6	1703.906
K7	1575.811
V8	1476.743
L9	1363.659
E10	1234.616
V11	1135.548
E12	978.474
S13	891.442
S14	804.410
D15	689.383
T16	588.335
I17	475.251
D18	360.224
N19	246.181
V20	147.113

b) ^{12}C K11(miscleavage) I13K K13(Ce)

log(e)	m+h	sequence
-4.4	2349.23950	iflk^7 TLTGKTKVLEVESSDTIDNVK^{27}akiq

mods: K13+Carboxyethyl

T L T G K T K V L E V E S S D T I D N V K

bond	+1y
T1	2248.192
L2	2135.108
T3	2034.060
G4	1977.039
K5	1848.944
T6	1747.896
K7	1547.780
V8	1448.711
L9	1335.627
E10	1206.585
V11	1107.516
E12	978.474
S13	891.442
S14	804.410
D15	689.383
T16	588.335
I17	475.251
D18	360.224
N19	246.181
V20	147.113

Figure 3.2| Peptide fragmentation pattern corresponding to carboxyethyl modification at a) K11 and b) K13. Complete list of modifications, mutations, and miscleavage events are stated in upper left corner. Matched y ions are listed in red.

Two lysine residues that were identified by LC-MS/MS for carboxyethyl modification are likely true positives, K33 and K48. Using the aforementioned approach for manual inspection of the MS2 data, it is clear that carboxyethyl K33 has been correctly assigned (Figure 3.2). The fragmentation pattern shows matched peptides throughout the entire peptide sequence and the log(e) score is good. Moreover, the peptides are also present with multiple ethylations, which is consistent with the data from chapter 3.1. Therefore, K33 can be accepted as a site of carboxyethyl modification.

The peptide corresponding to carboxyethyl K48 also has a thorough fragmentation pattern combined with a good log(e) score (Figure 3.3). This peptide is also observed with ethylations, which was expected based on the results using MALDI (chapter 3.1). Therefore K48 can also be accepted as a site of carboxyethyl modification.
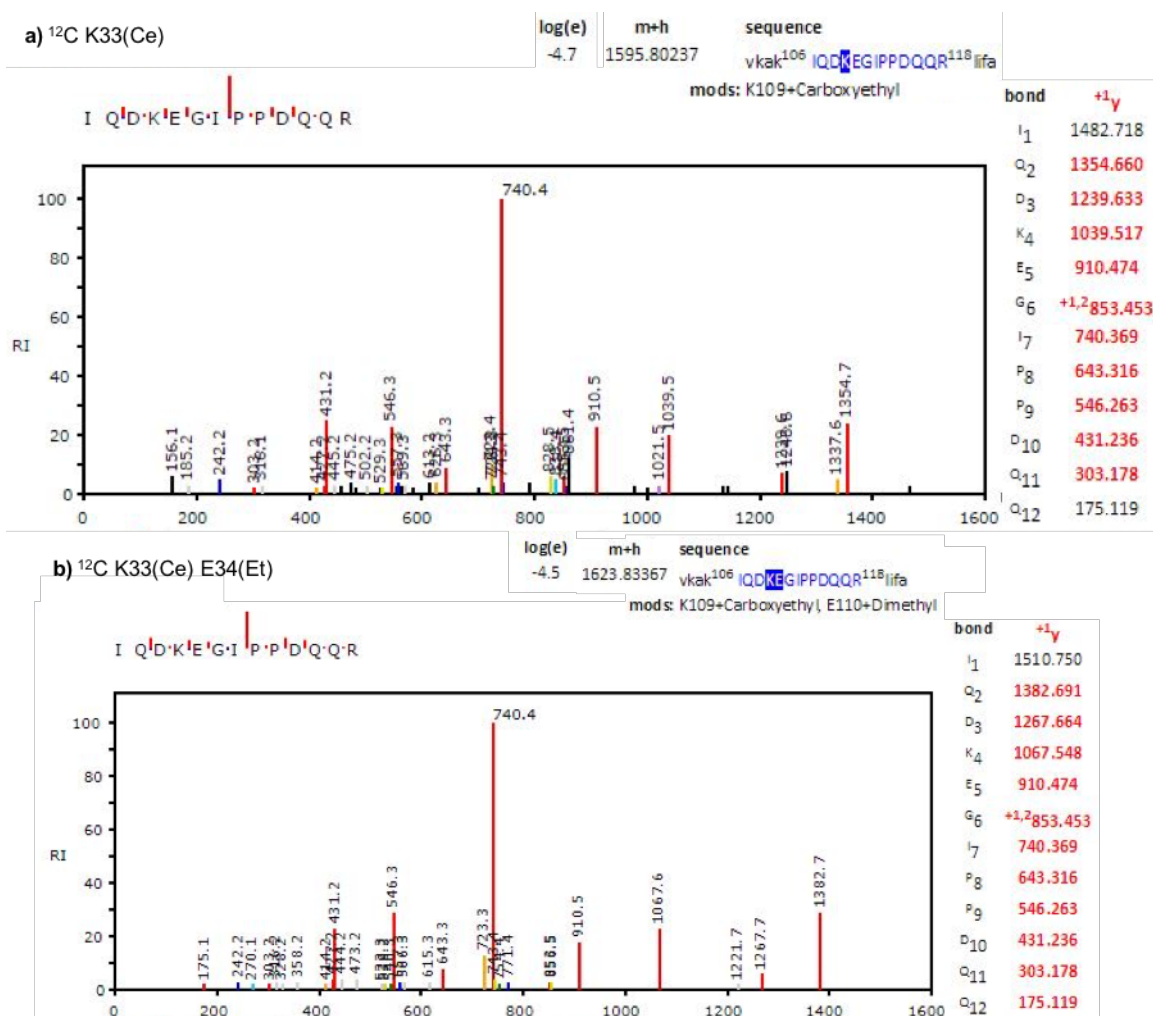
Figure 3.3| Peptide fragmentation pattern corresponding to carboxyethyl modification at K33 of human ubiquitin. a) K33 carboxyethyl modification. b) K33 carboxyethylation with ethylation at E34. Matched y ions are listed in red.

LC-MS/MS is a powerful tool for assigning the amino acid specific site of PTMs. Here, the importance of manually inspecting the MS2 data was highlighted in order to avoid accepting false positive results. From this it could also be confirmed that K33 and K48 are sites of carboxyethyl modification along the ubiquitin sequence. This is consistent with the results from the MALDI investigation and has enabled the specific modified residues to be defined. The results also demonstrate a consistency for sites of carboxyethyl modification between plant and human ubiquitin. Therefore the hypothesis of this investigation, that carboxyethyl modification of ubiquitin occurs at lysine residues, can be confirmed. Moreover it has been demonstrated that this modification specifically occurs at only two lysine residues.
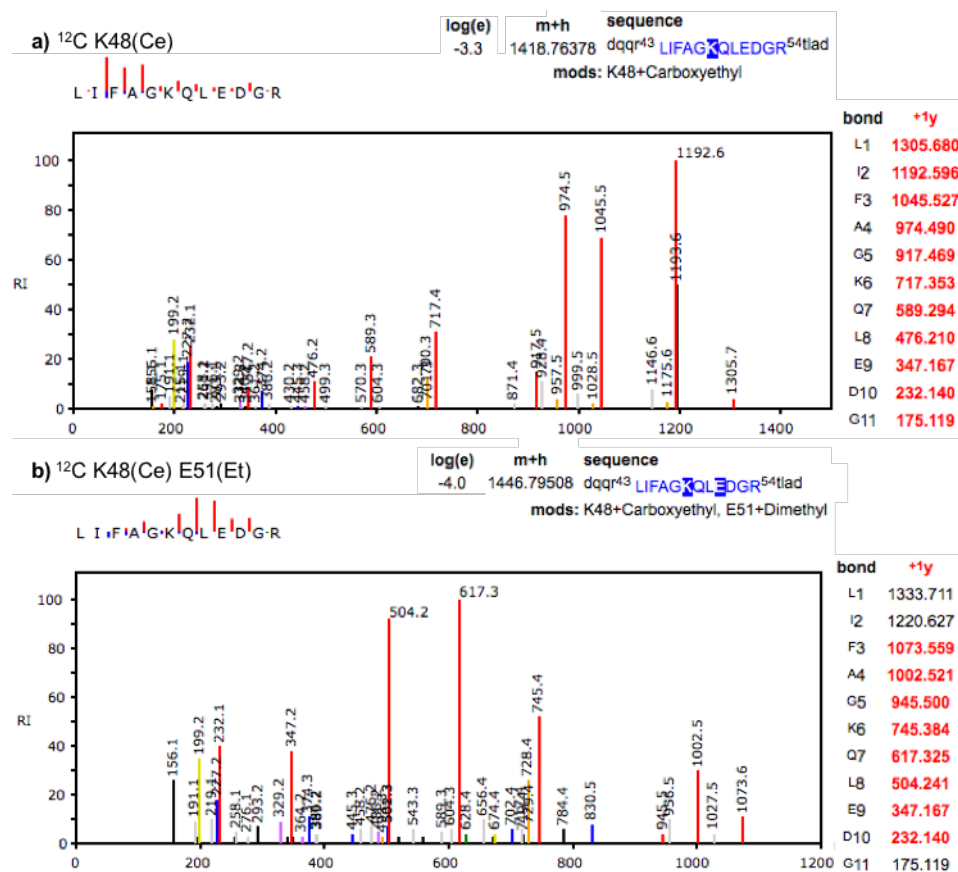
Figure 3.4| Peptide fragmentation pattern corresponding to peptides containing carboxyethyl modification of K48. Complete list of modifications are stated in upper left corner. Predicted y ion masses are listed with matched detected peptides in red.

3.4. Ubiquitin carboxyethyl modification is CO_2-dependent

In the previous investigation, it was demonstrated that K33 and K48 are sites of carboxyethyl modification (Chapter 3.2). Although this modification has a mass corresponding to a trapped carbamate, it has not been confirmed that the modification is CO_2-dependent. NMR studies utilise ^{13}C supplemented media to demonstrate formation of carbamate adducts from CO_2. It was therefore hypothesised that ^{13}C could be used to confirm the carboxyethyl modification is a CO_2-derived carbamate trapped by reaction with TEO. To achieve this the trapping reaction is supplemented with $NaH^{13}CO_3$, which will readily dissociate to form $^{13}CO_2$ and is subsequently ethylated during the reaction with TEO. Consequently, the carboxyethyl modification has a mass of 73.0244 Da. Subsequently, the peptides containing K33 and K48 were confirmed as sites of CO_2-dependent carboxyethyl modification.
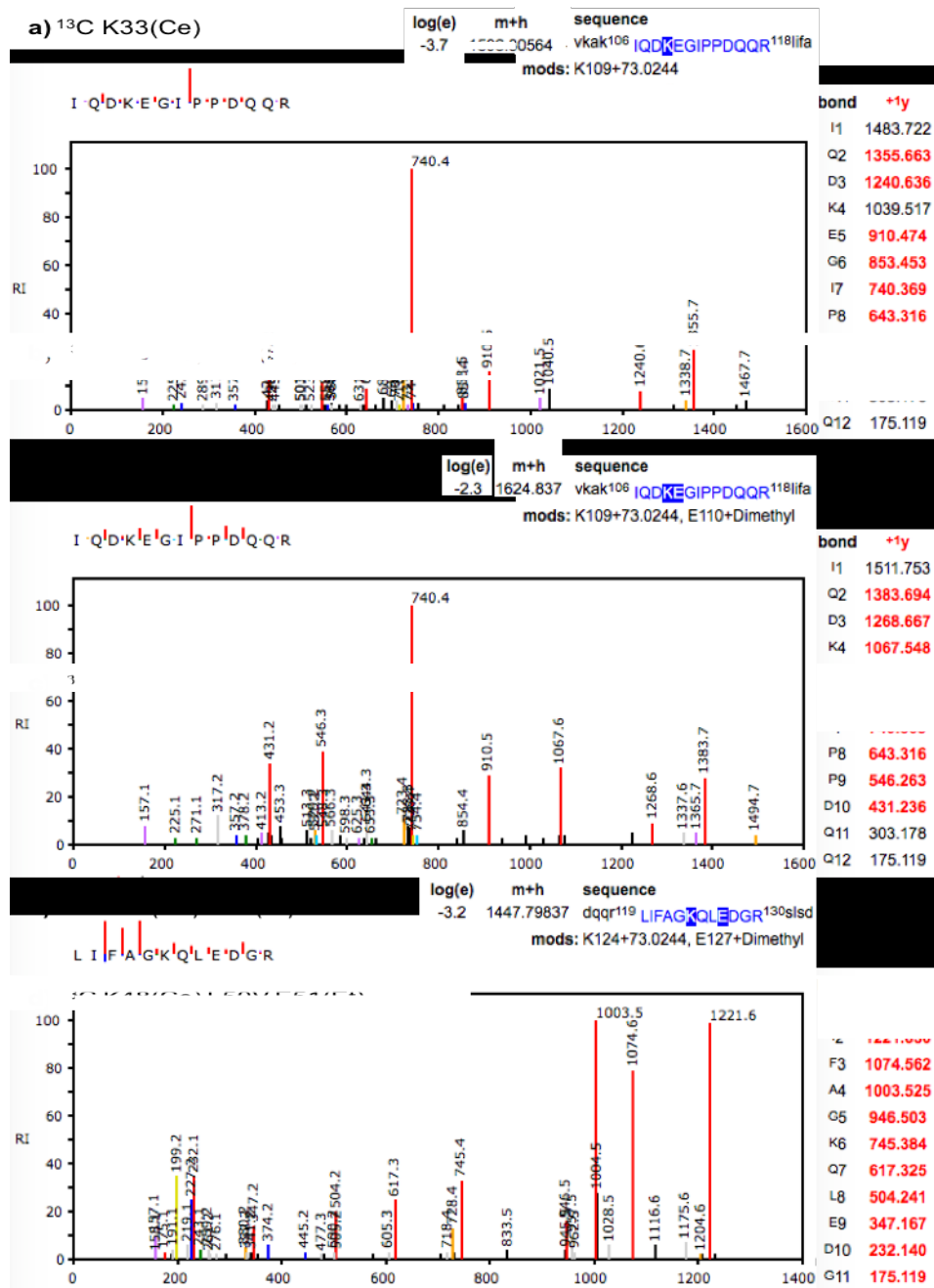
Figure 3.5| ^{13}C peptide fragmentation patterns corresponding to CO_2-dependent carboxyethyl modification of ubiquitin. **a)** carboxyethyl modification at K33. **b)** Carboxyethyl modification at K33 with ethylation at E34. **c)** Carboxyethyl modification at K48 with ethylation at E51. Predicted y ion masses are listed with matched detected peptides in red. Ce=Carboxyethylation, Et=Ethylation

The aim of this investigation was to use ^{13}C to demonstrate the carboxyethyl modification is CO_2-dependent. The trapping reaction was performed with 20 mM NaH^{13}CO$_3$, which was theorised to yield a carboxyethyl modification with a +1 Da shift

from that of the ^{12}C investigations. This resulted in identification of the peptides corresponding to carboxyethyl K33 and K48 (Figure 3.4). There is no matched peptide for the y ion of carboxyethyl K33 (Figure 3.4.A) but this is present for the peptide that includes ethylation at E34 (Figure 3.4.B). Despite this, the N terminal fragments (i.e. fragments including the carboxyethyl lysine residue) are matched y ions. This, combined with log(e) scores of -3.7 and -2.3, provides evidence in favour of a trapped CO_2-dependent carbamate at K33 of ubiquitin. In addition, the fragmentation patterns for carboxyethyl K48 contains matched peptides including and surrounding the modified lysine. This MS2 data has a log(e) score of -3.2, suggesting the carboxyethyl modification is due to a trapped CO_2-dependent carbamate.

Figure 3.6| MaxQuant MS2 data for 13C carboxyethyl a) K33 and b) K48 indicating carboxyethyl modification on the y10 and y7 ions, respectively.

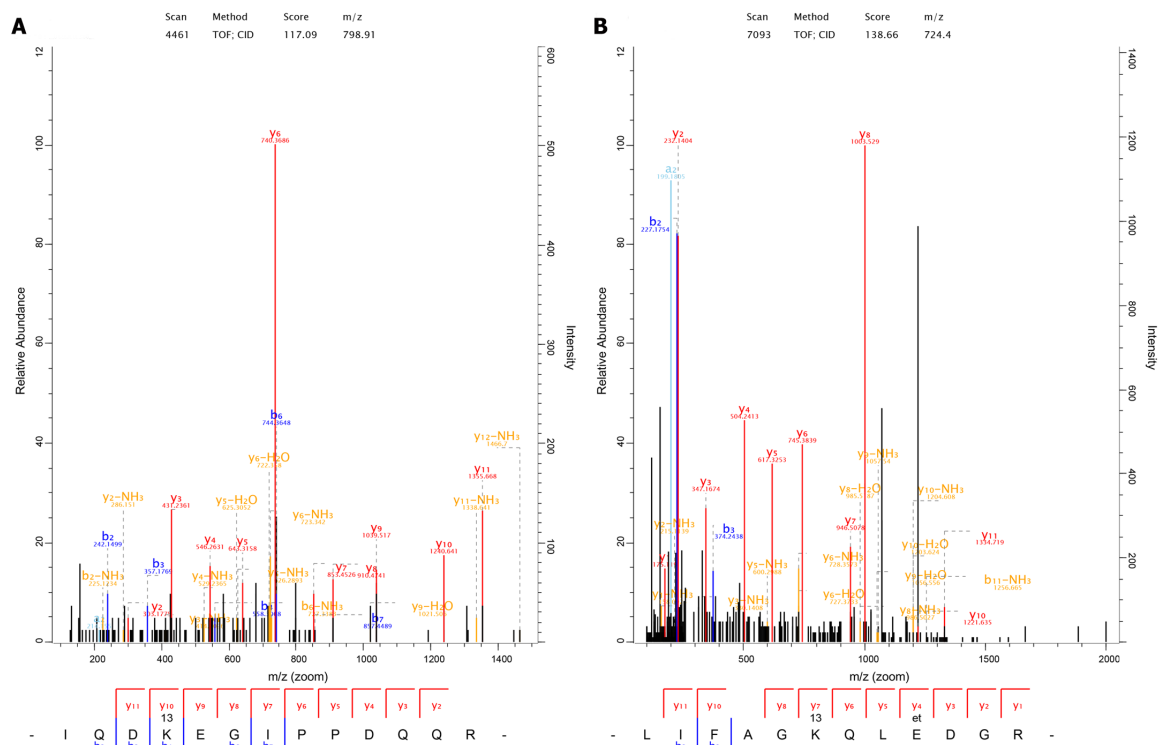Different software packages use alternative algorithms to assign a peptide mass to an entry in the proteome database. By using multiple software packages greater confidence can be achieved for peptides that have been matched with the differing algorithms. Consequently, the ^{13}C data was also processed in MaxQuant (Figure 3.5). This clearly shows matched peptides for the y ions of the carboxyethylated K33 and K48. In addition the high scores (117.09 and 138.66 for K33 and K48, respectively), provide greater confidence that these results are not due to chance, which is consistent with the results generated in X!Tandem. Modification of these lysine residues with a 73.0244 Da adduct requires the incorporation of a ^{13}CO$_2$ (44.9941 Da) and its alkylation during the trapping reaction, resulting in an additional ethyl (28.0303 Da) to this adduct. The reaction mixture was supplemented with NaH^{13}CO$_3$, which dissociated to form ^{13}CO$_2$. This, in turn, enabled the labile carbamate to form on these lysine residues. When compared to the trapping experiment using ^{12}C, the expected + 1.0033 Da mass shift of the modification, corresponding to the different carbon isotopes, is observed. Moreover, the ^{13}C modification is only observed at the residues previously identified as sites of ubiquitin carboxyethyl formation. Altogether, this investigation proved that the carboxyethyl modifications identified at K33 and K48 are due to carbamate formation derived from CO$_2$.

3.5. CO$_2$ inhibits ubiquitin discharge from E2 ligase.

The MS experiments have confirmed that CO$_2$ interacts with K33 and K48 of ubiquitin. However, the physiological significance of this interaction requires elucidation. Polyubiquitin chains are generated by the formation of isopeptide bonds between the Nε-Lysine on the substrate protein or ubiquitin and the carboxyl group of the C-terminal glycine residue of the next ubiquitin. Formation of a carbamate reverses the charge status of the Nε-amine group on lysine residues. Therefore, it was hypothesised that physiologically high CO$_2$ concentration will reduce the rate of polyubiqutin chain formation.

To test this hypothesis a previously established cross linking protocol was adapted and performed in the presence of 35 mM $NaHCO_3$ (Pickart and Raasi, 2005). Upon $NaHCO_3$ dissociation this equates to ~2 mM CO_2, which is observed in patients with chronic hypercapnia*. Under these conditions there are two mass shifts of the E2 ligase that correspond to the addition of mono- and di-ubiquitin chains (Figure 3.6). This effect is independent of increased cation concentration and boiling samples introduced protein bands at ~45 kDa. It is thought that these are artefactual polyubiquitin chains that cross link upon boiling (Pickart and Raasi, 2005).
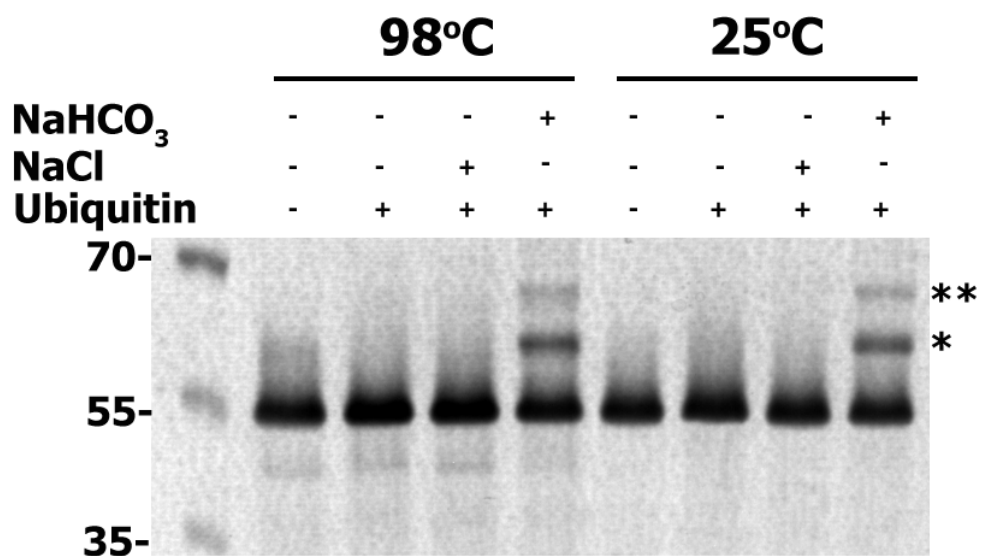
Figure 3.7| Ubiquitin~E2 discharge is perturbed by 2 mM CO_2. Ubiquitin discharge from E2 ligase is perturbed upon addition of 35 mM $NaHCO_3$, which dissociates to ~2 mM CO_2 at pH 7.5 and is independent of an increase in cation concentration. Resolved by SDS-PAGE, left four lanes represent boiled samples in Laemmli buffer. Right hand lanes represent samples incubated in Laemmli buffer at room temperature. Mass shifts observed are due to *) mono-ubiquitin and **) di-ubiquitin. n = 1.

Under conditions representing physiological hypercapnia there is a significant decrease in ubiquitin discharge from E2-25K (Figure 3.6). This resulted in the

formation of E2~Ub conjugates that are also observed by other groups investigating ubiquitylation kinetics (Buetow et al., 2015; Das et al., 2009; Saha et al., 2011). This suggests that carbamate formation at K48 disrupts ubiquitin discharge in a manner analogous to mutations that disrupt the stabilising interactions between E2 and Ubiquitin (Saha et al., 2011). Of note, none of these investigations report perturbed discharge of di-ubiquitin. This is because they perform experiments with a substrate protein whereas the experimental set up here does not. It will be necessary to perform a similar experiment and demonstrate that a) the rate of polyubiqutin chain formation is reduced, b) the effect of perturbed ubiquitin discharge is dose-dependent, c) carbamate stoichiometry correlates with the dose response, and d) the same effect is observed with K33. This information will prove useful when attempting to determine a physiologically relevant role for CO_2-dependent ubiquitin carbamylation. One possible role for this phenomenon is the reduction of proteasomal activity. The proteasome is a large complex that degrades proteins tagged with polyubiquitin chains. It has been demonstrated that substrate proteins tagged with tetraubiquitin chains are preferentially degraded by the proteasome (Singh et al., 2016). CO_2-mediated carbamate formation on K33 and K48 may reduce the activity of the proteasome by reducing ubiquitylation kinetics.

3.6. Conclusion of results

Here it has been demonstrated that K33 and K48 are sites of CO_2-dependent carbamate formation on ubiquitin. The use of TEO enabled the labile carbamate to be trapped and readily identified by MS. MALDI-TOF was originally used to confirm the presence of carboxyethylated peptides as part of an ethylation series before MS/MS data revealed the site of modification. Subsequently a ^{13}C investigation proved the modification is due to CO_2-dependent carbamate formation. This resulted in the conclusive assignment of K33 and K48 as sites of CO_2-mediated carbamylation. Despite this, a physiological role for this PTM has not yet been elucidated. However, initial investigations suggest carbamate formation reduces the rate of ubiquitin

discharge. Chapter 4 contains a more detailed discussion of these results and includes suggestions of future research.

4. Discussion

CO_2 has been demonstrated to have a signalling role in normal biological processes and disease (Cummins, 2017; Cummins and Keogh, 2016). CO_2 can interact with protein at uncharged amine groups to form a labile covalent modification called a carbamate (Ewing et al., 1980). This modification introduces a change of charge status that may have profound effects on protein interactions (Terrier and Douglas, 2010) or enable metal chelation for enzyme function (Lorimer et al., 1976). An alternative method for the stabilisation of carbamates is achieved by the positioning of positively charged residues in close proximity to the lysine residue interacting with CO_2 (Meigh et al., 2013). Thus, carbamate formation is known to exert an influence on the structure, function and activity of several proteins. Despite this, the number of known proteins to interact with CO_2 via carbamate formation is relatively low. This is largely due to the labile nature of carbamates preventing their identification by high throughput techniques. Therefore, the emphasis of previous research has been to identify effectors of CO_2-mediated signalling processes. The aim of this project was to identify a signalling molecule sensitive to fluctuating CO_2 levels. Previous work from this research group suggested ubiquitin was susceptible to carbamylation and, due to its known role in cellular signalling, was selected as the focus of this project (Linthwaite, 2016).

4.1. Mass spectrometry confirms ubiquitin is carbamylated at K33 and K48

A technique has been previously developed to enable identification of carbamates by MS (Linthwaite, 2016). This involves the ethylation of acidic residues by reaction with the alkylating reagent TEO, which traps carbamates onto the protein. Since glutamate and aspartate are also ethylated by the reaction with TEO, an ethylation series will be generated for each peptide. This is where a series of peptides are identified corresponding to all possible combinations of ethylation events, including the carboxyethyl modification indicative of the trapped carbamate. The initial investigation therefore aimed to verify carbamates that could be trapped and

identified by MS using MALDI-TOF. Two peptides were identified to incorporate a mass corresponding to a carboxyethyl modification as part of an ethylation series on Asp and Glu residues within the peptide (Table 3.1 and Table 3.2). This is a good indicator of the peptide containing a carboxyethylated residue but it does not confirm the site of modification.

LC MS/MS is used to assign PTM localizations. By taking this approach it was confirmed that K33 and K48 are sites of carboxyethylation on ubiquitin, along with ruling out false positive results. However, it was not formally possible to conclude that these modifications are due to CO_2. Therefore, an experiment was performed that utilised ^{13}C to demonstrate the modifications at K33 and K48 are CO_2-dependent trapped carbamates. Whilst this confirmed K33 and K48 as sites of CO_2 interaction, the physiological relevance of this modification is not clear. A limitation of the experimental setup is the inability to quantify the relative abundance of unmodified and carboxyethylated peptides. This is complicated by carboxyethylation resulting in miscleavage of the lysine residue.

Modification of ubiquitin lysine residues have been proposed to exert influence on subsequent ubiquitin modifications, including polyubiquitin chain synthesis (Ohtake et al., 2015). Here, acetylation of K6 and K48 are proposed to repress isopeptide bond formation between ubiquitin molecules at K11, K48 and K63. The inhibitory effect on polyubiquitin chain formation is proposed to be due to the hydrophobic property of the acetyl group attenuating interaction with ubiquitin binding proteins including the E2 and E3 ligases that perform chain elongation (Husnjak and Dikic, 2012; Ohtake et al., 2015). Since carbamylation reverses the charge status of lysine residues, it is possible that CO_2 exerts a similar effect on ubiquitin crosslinking to that of acetylation.

4.2. Physiological implications of ubiquitin carbamylation

Ubiquitin is an 8 kDa protein conserved throughout the eukaryotic kingdom. It is involved in a variety of cellular process ranging from protein tagging for degradation to signal transduction and DNA repair (Passmore and Barford, 2004). A variety of factors influence the process mediated by ubiquitination: ubiquitin polymerisation, cross-linking of specified lysine residues, ubiquitin chain branching and positioning of ubiquitin on the target protein (Sadowski and Sarcevic, 2010). In order for ubiquitin to bind to its target protein a series of reactions occur that result in formation of an isopeptide bond between the ubiquitin C-terminal glycine residue (G76) and the ε-amine group of a lysine residue of the substrate protein (Pickart, 2001). This process requires ATP and is catalysed by E1, E2, and E3 ubiquitin ligases (Finley and Chau, 1991; Jentsch, 1992). A protein bearing a single ubiquitin molecule is relatively stable, whilst proteins tagged with poly-ubiquitin chains are often rapidly degraded (Chau et al., 1989; Gregori et al., 1990; Singh et al., 2016). K48-linked poly-ubiquitin chains predominate and are the principle signal for 26S proteasomal degradation (Chau et al., 1989). However, ubiquitin contains 7 lysine residues and all of these may be utilised for poly-ubiquitin chain formation along with the N-terminal methionine (Peng et al., 2003). Specificity of cross-linked poly-ubiquitin chains is accomplished through particular E2/E3 pairing and the proximal environment that surrounds the lysine residues (Petroski and Deshaies, 2005; Sadowski and Sarcevic, 2010).

It has been demonstrated that K33 and K48 are sites of carbamylation. K33 linked ubiquitin is typically involved in non-proteolytic signalling processes. However, the extent of signalling performed by this atypical ubiquitin chain is poorly understood. Despite this, K33-linked ubiquitination has been implicated in the DNA damage response (Elia et al., 2015), AMPK signalling (Al-Hakim et al., 2008), TCR inactivation (Huang et al., 2010; Yang et al., 2015), repression of type I interferon transcription (Liu et al., 2018), recruitment to the pre-autophagosomal phagophore (Nibe et al., 2018), and post-golgi trafficking (Yuan et al., 2014). In contrast to K33, K48 linked ubiquitin is almost exclusively involved in targeting substrate proteins for degradation by the 26S

proteasome (Thrower et al., 2000). It is not yet clear how carbamylation of K33 and K48 affects these processes.

The results of the cross-linking assay suggest carbamylation of K48 reduces the rate of ubiquitylation. This is consistent with previous findings that report reduced ubiquitin kinetics upon destabilising interactions between ubiquitin and E2/E3 ligases (Saha et al., 2011). However this is in contrast to a recent report of increased ubiquitylation under hypercapnic conditions (Gwoździńska et al., 2017). It should be noted, however, that for this investigation Nedd-4 was used for ubiquitination assays. Nedd-4 is an E3 ligase that specifically catalyses K63-linked polyubiquitin chains (Maspero et al., 2013). Since carbamylation was only seen to occur at K33 and K48, it is unlikely that hypercapnia would reduce K63-linked polyubiquitination. In fact, carbamate formation may prevent crosslinking at these residues, which increases the probability of crosslinking at the remaining lysine residues (Ohtake et al., 2015).

Due to the reduced rate of ubiquitination it would be anticipated that an *in vivo* model would demonstrate reduced proteasomal activity. This is because proteins tagged with smaller ubiquitin chains are more stable than those with longer chains (Singh et al., 2016). Despite this, proteasomal activity has been reported to increase during hypercapnic conditions (Jaitovich et al., 2015; Ottenheijm et al., 2006). This may be explained by alternative CO_2-sensitive signalling pathways. Increased cAMP concentrations and PKA activation are both mechanisms through which proteasome phosphorylation is stimulated and this is correlated with enhanced proteasomal degradation (Lokireddy et al., 2015). It has previously been shown that elevated bicarbonate causes sAC to increase cAMP production and stimulate PKA activity (Lecuona et al., 2013; Townsend et al., 2009). Moreover, proteasomal inhibition has been reported to increase ER stress, induce aberrant signalling pathways and reduce *Drosophila* lifespan, with a compensatory mechanism afforded by increased autophagy (Suraweera et al., 2012; Velentzas et al., 2013). This provides a mechanism

through which hypercapnia mediates increased proteasome activity but questions remain concerning elevated CO_2 and rates of ubiquitination.

It has previously been reported that CO_2 may act as a readout for metabolic burden (Vadasz et al., 2012). Na^+/K^+ ATPase activity is reported to consume up to 40 % of cellular ATP therefore CO_2-responsive endocytosis of this membrane protein provides transient metabolic relief until CO_2 levels return to normal (Vadasz et al., 2012; Vadasz et al., 2007). This may also be the basis of an evolutionary conserved CO_2-responsive immune suppression (Helenius et al., 2009). Here the priority of the cell is survival to replication and reducing metabolic burden. As previously mentioned, proteasome activity is non-redundant (Suraweera et al., 2012; Velentzas et al., 2013). However, ubiquitylation, which costs ATP, is redundant since protein turnover by the proteasome can continue on previously ubiquitinated proteins. Upon return to basal CO_2 levels these dampened processes return to normal rates. In the context of chronic hypercapnia where ubiquitylation rates are reduced, expression of chaperones such as HSF1 may maintain proteostasis (Lu et al., 2018). This provides a mechanism through which the metabolic burden of the cell can be reduced without compromising essential homeostatic mechanisms.

The present study suggests K48-linked polyubiquitin chain formation would be decreased, which is in contrast to a previously published report that found K48-linked polyubiquitination was increased under hypercapnic conditions (Haegens et al., 2012). Such contradictory reports are commonplace when investigating the effect of hypercapnia. For example, NFκB is reported to be activated under elevated CO_2 conditions (Abolhassani et al., 2009; Oliver et al., 2012) but other findings report NFκB inactivation (Contreras et al., 2012; Helenius et al., 2009; Takeshita et al., 2003). There are also contrasting reports of p44/42 MAPK activation under hypercapnic conditions (Otulakowski et al., 2014; Welch et al., 2010). Thus, it is not surprising that the results of the cross-linking assay suggest an alternate role for carbamylated ubiquitin to that

of the literature. Further research is required to better understand the inconsistencies between published reports.

4.3. Future work

4.3.1. Carbamate stabilisation and Stoichiometry

Carbamates are a labile modification that typically require some form of stabilisation. This can be achieved through coordination of a metal ion (Lorimer and Miziorko, 1980), interaction with a proximal charged amine (Meigh et al., 2013), or because of the proximal environment providing a suitable pKa for carbamate stability (Jimenez-Morales et al., 2014). It is not known which of these is responsible for stabilisation of carbamates at K33 and K48 of ubiquitin, although it is unlikely that a carbamate is stabilised on ubiquitin through chelation of a metal ion. Structural studies investigating this will not only provide insights to the mechanism of carbamate stabilisation on ubiquitin but also to the general physicochemical properties of carbamate formation. This will impact the field by providing better predictive tools of proteins susceptible to carbamylation.

A CO_2 sensor must respond to fluctuating levels of CO_2. In order to understand this process, it is imperative to define carbamate stoichiometry at various CO_2 levels. This could be achieved in multiple ways. Firstly, use of an isobaric tag, such as TMT or iTRAQ, enables the relative quantification of carbamate formation at different CO_2 concentrations. This approach has been applied to other PTMs, such as phosphorylation (Glibert et al., 2015; Lim et al., 2017). Secondly, chemical modification of ubiquitin with an isotopic carboxyethyl group following the initial trapping experiment would enable the relative quantitation between the biological and chemical modifications. This approach has been performed in acetylation studies and has the advantage of reducing sample complexity (Gil et al., 2017). These approaches offer two complementary approaches to defining carbamate

stoichiometry under various conditions. It is expected that carbamylation of K33 and K48 relative to the unmodified peptide would change in a dose-dependent manner. However, a potential difficulty with the use of isobaric tags is that the unmodified peptide will be cleaved at K33 or K48. By taking the same approach as Gil et al. ubiquitin will be exclusively cleaved at arginine residues, thus streamlining the quantitation process.

4.3.2. *In vivo* applications

At present the trapping reagent can only be used *in vitro* or *ex vivo*. This makes it difficult to observe carbamylation in cellular contexts and therefore development of a cell membrane-permeable reagent is desired. Such a reagent would also ideally be optimised to enrich carbamylated proteins. Together, this would provide a workflow for enhanced identification of proteins susceptible to carbamylation, thus enabling identification of the 'carbamylome'. Until such a probe is developed, a proteomics investigation to identify more proteins susceptible to carbamylation could be achieved with SILAC. This is a technique that enables quantitative proteomics by labelling proteins *in vivo* with isotopic lysine and arginine residues. This permits up to three experimental conditions to be tested and for the proteins to be trapped *ex vivo*. Additionally, such an experimental setup could be used to observe the differing proteomes of cells exposed to hypercapnic or normocapnic conditions. A previous study compared two populations of eastern oysters that had been exposed to normocapnic or hypercapnic conditions. The authors of this study found that a relatively high proportion (12% of 456) of identified proteins were differentially expressed in hypercapnia (Tomanek et al., 2011). This study leaves room for improvement with regards investigating proteome depth and a proteomic analysis of mammalian cells exposed to varying levels of CO_2 could provide useful information regarding some of the previously described pathologies associated with hypercapnia. To this end, a similar strategy has been performed at the genome level, which identified an effector of CO_2 signalling pathways (Helenius et al., 2016a).

A possible *in vivo* experiment aimed at defining the dynamic arrangement of ubiquitin under elevated CO_2 is to expose cells to hypercapnic conditions and measure changes to ubiquitin pools using a protein standard absolute quantification assay (Kaiser et al., 2011). This would reveal key information regarding the effect of carbamate formation on ubiquitin crosslinking and the degree of substrate protein ubiquitination. Such insights would be better placed to provide information regarding the physiological relevance of carbamylation. Additionally, a novel fluorescence imaging technique, called PolyUb-FC, has been developed to inform investigators of polyubiquitin chain dynamics and potential interactors (Nibe et al., 2018). Since antibodies to atypical ubiquitin chains do not exist, it is not possible to derive this information from IP experiments for K33-linked chains.

4.3.3. *In vitro* applications for Ubiquitin kinetics

The formation of carbamates at K33 and K48 reverse the charge status of these residues. Research investigating other modifications at lysine residues of ubiquitin indicate that a change in charge status inhibits isopeptide bond formation (Ohtake et al., 2015). Because carbamylation is labile it is unlikely this modification fully inhibits isopeptide bond formation. It was therefore hypothesised that carbamylation at these sites reduces rate of isopeptide bond formation. A ubiquitin cross linking assay was performed using E2-25K, which exclusively cross links at K48 (David et al., 2010). Under hypercapnic conditions ubiquitin discharge from E2 is inhibited. However, dimer formation occurs, suggesting carbamate formation does not inhibit isopeptide bond formation. Therefore, it can be concluded that carbamate formation reduces the rate of polyubiquitin chain formation. This is in agreement with other research that demonstrate a change in charge status reduces the rate of ubiquitination but not ubiquitin binding affinity (Rodrigo-Brenni et al., 2010). The experimental setup here was limited to investigate K48 crosslinking at high CO_2 concentrations.

Due to time constraints it was not possible to complete the investigation of carbamate formation on ubiquitin kinetics. The future direction of this project would have been to consider the following:

- K33 was also identified as a site of carbamylation. It will be important to confirm the effect of carbamylation on K33-linked polyubiquitin chain formation.

- In a cellular context there are multiple E2 and E3 ligases that perform ubiquitin crosslinking at the 8 sites of cross linking. It would be informative to investigate whether carbamylation at K33 and K48 result in increased crosslinking of other residues.

- Within a cell a range of CO_2 concentrations will be experienced. It is anticipated that the rate of ubiquitination is dose dependant and that this would correlate with the stoichiometry of carbamylation at various CO_2 concentrations. To investigate this the cross-linking assay should be performed over a range of CO_2 concentrations. This investigation would complement a future mass spectrometry based assay to investigate carbamate stoichiometry

4.4. Conclusion

CO_2 is a fundamentally important to life. It is able to exert influence over cellular function through carbamylation of susceptible proteins involved in cell signalling pathways. Whilst many effects of elevated CO_2 in health and disease have been reported, not much is known regarding the CO_2 sensors. Therefore, the aim of this project was initially to identify a CO_2 sensor and define the mechanism through which CO_2-dependent regulation occurs. Due to time constraints, however, this was not performed to completion. A MS based approach defined K33 and K48 of ubiquitin as sites of carbamylation and a functional assay demonstrated the reduced rate of ubiquitination upon K48 carbamylation. This is consistent with other reports that observe reduced rates of ubiquitination upon a change of charge status to targeted lysine residues. The implications of this work are not clear but a potential role in

reducing metabolic burden has been outlined. Future work is required to better understand ubiquitin carbamylation. First, the factors governing carbamylation are poorly understood. It is not yet known what the occupancy of carbamylation is at various CO_2 concentrations or how the carbamate is stabilised. Second, the direct impact of elevated CO_2 on ubiquitin dynamics and its association with substrate proteins requires investigation. Finally, more information regarding ubiquitination kinetics of K33 and K48 is desired. Overall this project has provided evidence of a novel CO_2 sensor and provides a platform for future work to elucidate the physiological consequences of this interaction.

5. Bibliography

Abolhassani, M., Guais, A., Chaumet-Riffaud, P., Sasco, A.J., and Schwartz, L. (2009). Carbon dioxide inhalation causes pulmonary inflammation. Am J Physiol Lung Cell Mol Physiol *296*, L657-665.

Abraham, S.J., Kobayashi, T., Solaro, R.J., and Gaponenko, V. (2009). Differences in lysine pKa values may be used to improve NMR signal dispersion in reductively methylated proteins. J Biomol NMR *43*, 239-246.

Adijanto, J., Banzon, T., Jalickee, S., Wang, N.S., and Miller, S.S. (2009). CO_2-induced ion and fluid transport in human retinal pigment epithelium. J Gen Physiol *133*, 603-622.

Al-Hakim, A.K., Zagorska, A., Chapman, L., Deak, M., Peggie, M., and Alessi, D.R. (2008). Control of AMPK-related kinases by USP9X and atypical Lys(29)/Lys(33)-inked polyubiquitin chains. Biochem J *411*, 249-260.

Alkalay, I., Yaron, A., Hatzubai, A., Orian, A., Ciechanover, A., and Ben-Neriah, Y. (1995). Stimulation-dependent I-kappa-B-alpha phosphorylation marks the NF-kappa-B inhibitor for degradation via the ubiquitin-proteasome pathway. Proceedings of the National Academy of Sciences of the United States of America *92*, 10599-10603.

Amato, M.B.P., Barbas, C.S.V., Medeiros, D.M., Magaldi, R.B., Schettino, G.D.P., Lorenzi, G., Kairalla, R.A., Deheinzelin, D., Munoz, C., Oliveira, R*., et al.* (1998). Effect of a protective-ventilation strategy on mortality in the acute respiratory distress syndrome. New England Journal of Medicine *338*, 347-354.

Baeuerle, P.A., and Baltimore, D. (1988). Activation of DNA-binding activity in an apparently cytoplasmic precursor of the NF-kappa-B transcription factor. Cell *53*, 211-217.

Beg, A.A., Finco, T.S., Nantermet, P.V., and Baldwin, A.S. (1993). Tumor-necrosis-factor and interleukin-1 lead to phosphorylation and loss of I-kappa-B-alpha - a mechanism for NF-kappa-B activation. Molecular and Cellular Biology *13*, 3301-3310.

Benning, M.M., Shim, H., Raushel, F.M., and Holden, H.M. (2001). High resolution X-ray structures of different metal-substituted forms of phosphotriesterase from Pseudomonas diminuta. Biochemistry *40*, 2712-2722.

Blombach, B., and Takors, R. (2015). CO_2-Intrinsic Product, Essential Substrate, and Regulatory Trigger of Microbial and Mammalian Production Processes. Frontiers in bioengineering and biotechnology *3*, 108-108.

Boron, W.F., Endeward, V., Gros, G., Musa-Aziz, R., and Pohl, P. (2011). Intrinsic CO_2 Permeability of Cell Membranes and Potential Biological Relevance of CO_2 Channels. ChemPhysChem *12*, 1017-1019.

Briva, A., Vadasz, I., Lecuona, E., Welch, L.C., Chen, J., Dada, L.A., Trejo, H.E., Dumasius, V., Azzam, Z.S., Myrianthefs, P.M*., et al.* (2007). High CO_2 levels impair alveolar epithelial function independently of pH. PloS one *2*, e1238.

Brown, K., Gerstberger, S., Carlson, L., Franzoso, G., and Siebenlist, U. (1995). Control of I-kappa-B-alpha proteolysis by site-specific, signal-induced phosphorylation. Aids Res Hum Retrovir *11*, S118-S118.

Brown, K., Park, S., Kanno, T., Franzoso, G., and Siebenlist, U. (1993). Mutual regulation of the transcriptional activator NF-kappa-B and its inhibitor, I-kappa-B-alpha. Proceedings of the National Academy of Sciences of the United States of America *90*, 2532-2536.

Brzovic, P.S., Lissounov, A., Christensen, D.E., Hoyt, D.W., and Klevit, R.E. (2006). A UbcH5/ubiquitin noncovalent complex is required for processive BRCA1-directed ubiquitination. Mol Cell *21*, 873-880.

Buetow, L., Gabrielsen, M., Anthony, N.G., Dou, H., Patel, A., Aitkenhead, H., Sibbet, G.J., Smith, B.O., and Huang, D.T. (2015). Activation of a primed RING E3-E2-ubiquitin complex by non-covalent ubiquitin. Mol Cell *58*, 297-310.

Cardozo, T., and Pagano, M. (2004). The SCF ubiquitin ligase: Insights into a molecular machine. Nature Reviews Molecular Cell Biology *5*, 739-751.

Carvalho, A.F., Pinto, M.P., Grou, C.P., Vitorino, R., Domingues, P., Yamao, F., Sa-Miranda, C., and Azevedo, J.E. (2012). High-Yield Expression in Escherichia coli and Purification of Mouse Ubiquitin-Activating Enzyme E1. Mol Biotechnol *51*, 254-261.

Celli, B.R., Cote, C.G., Marin, J.M., Casanova, C., Montes de Oca, M., Mendez, R.A., Pinto Plata, V., and Cabral, H.J. (2004). The body-mass index, airflow obstruction, dyspnea, and exercise capacity index in chronic obstructive pulmonary disease. New Engl J Med *350*, 1005-1012.

Chau, V., Tobias, J.W., Bachmair, A., Marriott, D., Ecker, D.J., Gonda, D.K., and Varshavsky, A. (1989). A multiubiquitin chain is confined to specific lysine in a targeted short-lived protein. Science *243*, 1576-1583.

Chen, J.G., Sandberg, M., and Weber, S.G. (1993). Chromatographic method for the determination of conditional equilibrium-constants for the carbamate formation reaction from amino-acids and peptides in aqueous-solution. J Am Chem Soc *115*, 7343-7350.

Chen, Z.J. (2005). Ubiquitin signalling in the NF-kappaB pathway. Nat Cell Biol *7*, 758-765.

Chen, Z.J., Hagler, J., Palombella, V.J., Melandri, F., Scherer, D., Ballard, D., and Maniatis, T. (1995). Signal-induced site-specific phosphorylation targets I-kappa-B-alpha to the ubiquitin-proteasome pathway. Genes & Development *9*, 1586-1597.

Cleland, W.W., Andrews, T.J., Gutteridge, S., Hartman, F.C., and Lorimer, G.H. (1998). Mechanism of Rubisco: The carbamate as general base. Chemical Reviews *98*, 549-561.

Contreras, M., Ansari, B., Curley, G., Higgins, B.D., Hassett, P., O'Toole, D., and Laffey, J.G. (2012). Hypercapnic acidosis attenuates ventilation-induced lung injury by a nuclear factor-kappa B dependent mechanism. Crit Care Med *40*, 2622-2630.

Cook, Z.C., Gray, M.A., and Cann, M.J. (2012). Elevated carbon dioxide blunts mammalian cAMP signaling dependent on inositol 1,4,5-triphosphate receptor-mediated Ca2+ release. The Journal of biological chemistry *287*, 26291-26301.

Cummins, E.P. (2017). Physiological gases in health and disease - key regulatory factors, not just a lot of hot air. Journal of Physiology-London *595*, 2421-2422.

Cummins, E.P., and Keogh, C.E. (2016). Respiratory gases and the regulation of transcription. Exp Physiol *101*, 986-1002.

Cummins, E.P., Oliver, K.M., Lenihan, C.R., Fitzpatrick, S.F., Bruning, U., Scholz, C.C., Slattery, C., Leonard, M.O., McLoughlin, P., and Taylor, C.T. (2010). NF-kappa B Links CO_2 Sensing to Innate Immunity and Inflammation in Mammalian Cells. Journal of Immunology *185*, 4439-4445.

Cummins, E.P., Selfridge, A.C., Sporn, P.H., Sznajder, J.I., and Taylor, C.T. (2014). Carbon dioxide-sensing in organisms and its implications for human disease. Cellular and Molecular Life Sciences *71*, 831-845.

Das, R., Mariano, J., Tsai, Y.C., Kalathur, R.C., Kostova, Z., Li, J., Tarasov, S.G., McFeeters, R.L., Altieri, A.S., Ji, X.*, et al.* (2009). Allosteric activation of E2-RING finger-mediated ubiquitylation by a structurally defined specific E2-binding region of gp78. Mol Cell *34*, 674-685.

David, Y., Ziv, T., Admon, A., and Navon, A. (2010). The E2 Ubiquitin-conjugating Enzymes Direct Polyubiquitination to Preferred Lysines. Journal of Biological Chemistry *285*, 8595-8604.

de Wolf, E., Cook, J., and Dale, N. (2017). Evolutionary adaptation of the sensitivity of connexin26 hemichannels to CO_2. Proc R Soc B-Biol Sci *284*, 7.

Deshaies, R.J. (1999). SCF and cullin/RING H2-based ubiquitin ligases. Annu Rev Cell Dev Biol *15*, 435-467.

Dick, L.A., Heibel, G., Moore, E.G., and Spiro, T.G. (1999). UV resonance Raman spectra reveal a structural basis for diminished proton and CO_2 binding to alpha,alpha-cross-linked hemoglobin. Biochemistry *38*, 6406-6410.

Elia, A.E., Boardman, A.P., Wang, D.C., Huttlin, E.L., Everley, R.A., Dephoure, N., Zhou, C., Koren, I., Gygi, S.P., and Elledge, S.J. (2015). Quantitative Proteomic Atlas of Ubiquitination and Acetylation in the DNA Damage Response. Mol Cell *59*, 867-881.

Ewing, S.P., Lockshon, D., and Jencks, W.P. (1980). Mechanism of cleavage of carbamate anions. J Am Chem Soc *102*, 3072-3084.

Finley, D., and Chau, V. (1991). Ubiquitination. Annu Rev Cell Biol *7*, 25-69.

Fong, A., and Sun, S.C. (2002). Genetic evidence for the essential role of beta-transducin repeat-containing protein in the inducible processing of NF-kappa B2/p100. Journal of Biological Chemistry *277*, 22111-22114.

Frommer, W.B. (2010). CO($_2$)mmon Sense. Science *327*, 275-276.

Gil, J., Ramirez-Torres, A., Chiappe, D., Luna-Penaloza, J., Fernandez-Reyes, F.C., Arcos-Encarnacion, B., Contreras, S., and Encarnacion-Guevara, S. (2017). Lysine

acetylation stoichiometry and proteomics analyses reveal pathways regulated by sirtuin 1 in human cells. The Journal of biological chemistry.

Glass, D.J. (2005). Skeletal muscle hypertrophy and atrophy signaling pathways. Int J Biochem Cell Biol *37*, 1974-1984.

Glibert, P., Meert, P., Van Steendam, K., Martens, L., Deforce, D., and Dhaenens, M. (2015). Phospho-iTRAQ data article: Assessing isobaric labels for the large-scale study of phosphopeptide stoichiometry. Data in brief *4*, 60-65.

Golemi, D., Maveyraud, L., Vakulenko, S., Samama, J.P., and Mobashery, S. (2001). Critical involvement of a carbamylated lysine in catalytic function of class D beta-lactamases. Proc Natl Acad Sci U S A *98*, 14280-14285.

Gregori, L., Poosch, M.S., Cousins, G., and Chau, V. (1990). A uniform isopeptide-linked multiubiquitin chain is sufficient to target substrate for degradation in ubiquitin-mediated proteolysis. Journal of Biological Chemistry *265*, 8354-8357.

Gutknecht, J., Bisson, M.A., and Tosteson, F.C. (1977). Diffusion of carbon-dioxide through lipid bilayer membranes - effects of carbonic-anhydrase, bicarbonate, and unstirred layers. Journal of General Physiology *69*, 779-794.

Gwoździńska, P., Buchbinder, B.A., Mayer, K., Herold, S., Morty, R.E., Seeger, W., and Vadász, I. (2017). Hypercapnia Impairs ENaC Cell Surface Stability by Promoting Phosphorylation, Polyubiquitination and Endocytosis of β-ENaC in a Human Alveolar Epithelial Cell Line. Front Immunol *8*. 591

Hackling, M.W., and Garnett, P.J. (1985). Misconceptions of chemical-equilibrium. European Journal of Science Education *7*, 205-214.

Haegens, A., Schols, A.M., Gorissen, S.H., van Essen, A.L., Snepvangers, F., Gray, D.A., Shoelson, S.E., and Langen, R.C. (2012). NF-kappa B activation and polyubiquitin conjugation are required for pulmonary inflammation-induced diaphragm atrophy. Am J Physiol-Lung Cell Mol Physiol *302*, L103-L110.

Hailfinger, S., Lenz, G., Ngo, V., Posvitz-Fejfar, A., Rebeaud, F., Guzzardi, M., Penas, E.-M.M., Dierlamm, J., Chan, W.C., Staudt, L.M.*, et al.* (2009). Essential role of MALT1 protease activity in activated B cell-like diffuse large B-cell lymphoma. Proceedings of the National Academy of Sciences of the United States of America *106*, 19946-19951.

Hall, P.R., Zheng, R., Antony, L., Pusztai-Carey, M., Carey, P.R., and Yee, V.C. (2004). Transcarboxylase 5S structures: assembly and catalytic mechanism of a multienzyme complex subunit. EMBO J *23*, 3621-3631.

Hampe, E.M., and Rudkevich, D.M. (2003). Exploring reversible reactions between CO_2 and amines. Tetrahedron *59*, 9619-9625.

Hanly, E.J., Fuentes, J.M., Aurora, A.R., Bachman, S.L., De Maio, A., Marohn, M.R., and Talamini, M.A. (2006). Carbon dioxide pneumoperitoneum prevents mortality from sepsis. Surgical Endoscopy and Other Interventional Techniques *20*, 1482-1487.

Heissmeyer, V., Krappmann, D., Hatada, E.N., and Scheidereit, C. (2001). Shared pathways of I kappa B kinase-induced SCF beta TrCP-mediated ubiquitination and

degradation for the NF-kappa B precursor p105 and I kappa B alpha. Molecular and Cellular Biology *21*, 1024-1035.

Helenius, I.T., Haake, R.J., Kwon, Y.J., Hu, J.A., Krupinski, T., Casalino-Matsuda, S.M., Sporn, P.H.S., Sznajder, J.I., and Beitel, G.J. (2016a). Identification of Drosophila Zfh2 as a Mediator of Hypercapnic Immune Regulation by a Genome-Wide RNA Interference Screen. Journal of Immunology *196*, 655-667.

Helenius, I.T., Krupinski, T., Turnbull, D.W., Gruenbaum, Y., Silverman, N., Johnson, E.A., Sporn, P.H.S., Sznajder, J.I., and Beitel, G.J. (2009). Elevated CO_2 suppresses specific Drosophila innate immune responses and resistance to bacterial infection. Proceedings of the National Academy of Sciences of the United States of America *106*, 18710-18715.

Helenius, I.T., Nair, A., Bittar, H.E.T., Sznajder, J.I., Sporn, P.H.S., and Beitel, G.J. (2016b). Focused Screening Identifies Evoxine as a Small Molecule That Counteracts CO_2-Induced Immune Suppression. J Biomol Screen *21*, 363-371.

Henkel, T., Machleidt, T., Alkalay, I., Kronke, M., Ben-Neriah, Y., and Baeuerle, P.A. (1993). Rapid proteolysis of I-kappa-B-alpha is necessary for activation of transcription factor NF-kappa-B. Nature *365*, 182-185.

Hetherington, A.M., and Raven, J.A. (2005). The biology of carbon dioxide. Current Biology *15*, R406-R410.

Hsia, C.C.W. (1998). Mechanisms of disease - Respiratory function of hemoglobin. New England Journal of Medicine *338*, 239-247.

Huang, H.N., Jeon, M.S., Liao, L.J., Yang, C., Elly, C., Yates, J.R., and Liu, Y.C. (2010). K33-Linked Polyubiquitination of T Cell Receptor-zeta Regulates Proteolysis-Independent T Cell Signaling. Immunity *33*, 60-70.

Huckstepp, R.T., and Dale, N. (2011). CO_2-dependent opening of an inwardly rectifying K+ channel. Pflugers Arch *461*, 337-344.

Huckstepp, R.T.R., Bihi, R.I., Eason, R., Spyer, K.M., Dicke, N., Willecke, K., Marina, N., Gourine, A.V., and Dale, N. (2010a). Connexin hemichannel-mediated CO_2-dependent release of ATP in the medulla oblongata contributes to central respiratory chemosensitivity. Journal of Physiology-London *588*, 3901-3920.

Huckstepp, R.T.R., Eason, R., Sachdev, A., and Dale, N. (2010b). CO_2-dependent opening of connexin 26 and related beta connexins. Journal of Physiology-London *588*, 3921-3931.

Husnjak, K., and Dikic, I. (2012). Ubiquitin-binding proteins: decoders of ubiquitin-mediated cellular functions. Annu Rev Biochem *81*, 291-322.

Jaitovich, A., Angulo, M., Lecuona, E., Dada, L.A., Welch, L.C., Cheng, Y., Gusarova, G., Ceco, E., Liu, C., Shigemura, M.*, et al.* (2015). High CO_2 Levels Cause Skeletal Muscle Atrophy via AMP-activated Kinase (AMPK), FoxO3a Protein, and Muscle-specific Ring Finger Protein 1 (MuRF1). Journal of Biological Chemistry *290*, 9183-9194.

Jentsch, S. (1992). Ubiquitin-dependent protein degradation: a cellular perspective. Trends in cell biology *2*, 98-103.

Jimenez-Morales, D., Adamian, L., Shi, D.S., and Liang, J. (2014). Lysine carboxylation: unveiling a spontaneous post-translational modification. Acta Crystallogr Sect D-Struct Biol *70*, 48-57.

Joshi, H.M., and Tabita, F.R. (1996). A global two component signal transduction system that integrates the control of photosynthesis, carbon dioxide assimilation, and nitrogen fixation. Proceedings of the National Academy of Sciences of the United States of America *93*, 14515-14520.

Kaiser, S.E., Riley, B.E., Shaler, T.A., Trevino, R.S., Becker, C.H., Schulman, H., and Kopito, R.R. (2011). Protein standard absolute quantification (PSAQ) method for the measurement of cellular ubiquitin pools. Nat Methods *8*, 691-U129.

Karin, M., and Ben-Neriah, Y. (2000). Phosphorylation meets ubiquitination: The control of NF-kappa B activity. Annual Review of Immunology *18*, 621-+.

Keogh, C.E., Scholz, C.C., Rodriguez, J., Selfridge, A.C., von Kriegsheim, A., and Cummins, E.P. (2017). Carbon dioxide-dependent regulation of NF-kappa B family members RelB and p100 gives molecular insight into CO_2-dependent immune regulation. Journal of Biological Chemistry *292*, 11561-11571.

Khalifah, R.G. (1973). Carbon-dioxide hydration activity of carbonic-anhydrase - paradoxical consequences of unusually rapid catalysis. Proceedings of the National Academy of Sciences of the United States of America *70*, 1986-1989.

Kilmartin, J.V., Fogg, J., Luzzana, M., and Rossiber.L (1973). Role of alpha-amino groups of alpha and beta chains of human hemoglobin in oxygen-linked binding of carbon-dioxide. Journal of Biological Chemistry *248*, 7039-7043.

Laffey, J.G., Honan, D., Hopkins, N., Hyvelin, J.M., Boylan, J.F., and McLoughlin, P. (2004). Hypercapnic acidosis attenuates endotoxin-induced acute lung injury. Am J Respir Crit Care Med *169*, 46-56.

Lecuona, E., Sun, H., Chen, J., Trejo, H.E., Baker, M.A., and Sznajder, J.I. (2013). Protein kinase A-Ialpha regulates Na,K-ATPase endocytosis in alveolar epithelial cells exposed to high CO_2) concentrations. American journal of respiratory cell and molecular biology *48*, 626-634.

Leidner, U., Palkowitsch, L., Marienfeld, U., Fischer, D., and Marienfeld, R. (2008). Identification of lysine residues critical for the transcriptional activity and polyubiquitination of the NF-kappa B family member RelB. Biochem J *416*, 117-127.

Lim, M.Y., O'Brien, J., Paulo, J.A., and Gygi, S.P. (2017). Improved Method for Determining Absolute Phosphorylation Stoichiometry Using Bayesian Statistics and Isobaric Labeling. Journal of proteome research *16*, 4217-4226.

Lindskog, S. (1997). Structure and mechanism of carbonic anhydrase. Pharmacology & Therapeutics *74*, 1-20.

Linthwaite, V. (2016). Development of a novel proteomics tool for the discovery of unknown carbamates (University of Durham), p. 240.

Liu, S., Jiang, M., Wang, W., Liu, W., Song, X., Ma, Z., Zhang, S., Liu, L., Liu, Y., and Cao, X. (2018). Nuclear RNF2 inhibits interferon function by promoting K33-linked STAT1 disassociation from DNA. Nat Immunol *19*, 41-52.

Lokireddy, S., Kukushkin, N.V., and Goldberg, A.L. (2015). cAMP-induced phosphorylation of 26S proteasomes on Rpn6/PSMD11 enhances their activity and the degradation of misfolded proteins. Proc Natl Acad Sci U S A *112*, E7176-7185.

Lorimer, G.H. (1983). Carbon-dioxide and carbamate formation - the makings of a biochemical control-system. Trends in Biochemical Sciences *8*, 65-68.

Lorimer, G.H., Badger, M.R., and Andrews, T.J. (1976). Activation of ribulose-1,5-bisphosphate carboxylase by carbon-dioxide and magnesium-ions - equilibria, kinetics, a suggested mechanism, and physiological implications. Biochemistry *15*, 529-536.

Lorimer, G.H., and Miziorko, H.M. (1980). Carbamate formation on the epsilon-amino group of a lysyl residue as the basis for the activation of ribulosebisphosphate carboxylase by CO_2 and mg2+. Biochemistry *19*, 5321-5328.

Lu, Z., Casalino-Matsuda, S.M., Nair, A., Buchbinder, A., Budinger, G.R.S., Sporn, P.H.S., and Gates, K.L. (2018). A role for heat shock factor 1 in hypercapnia-induced inhibition of inflammatory cytokine expression. FASEB J, fj201701164R.

Marienfeld, R., Berberich-Siebelt, F., Berberich, I., Denk, A., Serfling, E., and Neumann, M. (2001). Signal-specific and phosphorylation-dependent RelB degradation: a potential mechanism of NF-kappa B control. Oncogene *20*, 8142-8147.

Maspero, E., Valentini, E., Mari, S., Cecatiello, V., Soffientini, P., Pasqualato, S., and Polo, S. (2013). Structure of a ubiquitin-loaded HECT ligase reveals the molecular basis for catalytic priming. Nat Struct Mol Biol *20*, 696-701.

Matsuda, N. (2016). Phospho-ubiquitin: upending the PINK-Parkin-ubiquitin cascade. J Biochem *159*, 379-385.

Matthay, M.A., Folkesson, H.G., and Clerici, C. (2002). Lung epithelial fluid transport and the resolution of pulmonary edema. Physiol Rev *82*, 569-600.

Matthew, J.B., Morrow, J.S., Wittebort, R.J., and Gurd, F.R. (1977). Quantitative determination of carbamino adducts of alpha and beta chains in human adult hemoglobin in presence and absence of carbon monoxide and 2,3-diphosphoglycerate. The Journal of biological chemistry *252*, 2234-2244.

Maveyraud, L., Golemi, D., Kotra, L.P., Tranier, S., Vakulenko, S., Mobashery, S., and Samama, J.P. (2000). Insights into class D beta-lactamases are revealed by the crystal structure of the OXA10 enzyme from Pseudomonas aeruginosa. Structure *8*, 1289-1298.

Meigh, L., Greenhalgh, S.A., Rodgers, T.L., Cann, M.J., Roper, D.I., and Dale, N. (2013). CO_2 directly modulates connexin 26 by formation of carbamate bridges between subunits. Elife *2*, 13.

Morollo, A.A., Petsko, G.A., and Ringe, D. (1999). Structure of a Michaelis complex analogue: propionate binds in the substrate carboxylate site of alanine racemase. Biochemistry *38*, 3293-3301.

Moroney, J.V., Bartlett, S.G., and Samuelsson, G. (2001). Carbonic anhydrases in plants and algae. Plant Cell Environ *24*, 141-153.

Neumann, M., Klar, S., Wilisch-Neumann, A., Hollenbach, E., Kavuri, S., Leverkus, M., Kandolf, R., Brunner-Weinzierl, M.C., and Klingel, K. (2011). Glycogen synthase kinase-3 beta is a crucial mediator of signal-induced RelB degradation. Oncogene *30*, 2485-2492.

Nibe, Y., Oshima, S., Kobayashi, M., Maeyashiki, C., Matsuzawa, Y., Otsubo, K., Matsuda, H., Aonuma, E., Nemoto, Y., Nagaishi, T.*, et al.* (2018). Novel polyubiquitin imaging system, PolyUb-FC, reveals that K33-linked polyubiquitin is recruited by SQSTM1/p62. Autophagy, 1-12.

Nichol, A.D., O'Cronin, D.F., Howell, K., Naughton, F., O'Brien, S., Boylan, J., O'Connor, C., O'Toole, D., Laffey, J.G., and McLoughlin, P. (2009). Infection-induced lung injury is worsened after renal buffering of hypercapnic acidosis. Crit Care Med *37*, 2953-2961.

Ohtake, F., Saeki, Y., Sakamoto, K., Ohtake, K., Nishikawa, H., Tsuchiya, H., Ohta, T., Tanaka, K., and Kanno, J. (2015). Ubiquitin acetylation inhibits polyubiquitin chain elongation. EMBO Rep *16*, 192-201.

Oliver, K.M., Lenihan, C.R., Bruning, U., Cheong, A., Laffey, J.G., McLoughlin, P., Taylor, C.T., and Cummins, E.P. (2012). Hypercapnia Induces Cleavage and Nuclear Localization of RelB Protein, Giving Insight into CO_2 Sensing and Signaling. Journal of Biological Chemistry *287*, 14004-14011.

Orian, A., Gonen, H., Bercovich, B., Fajerman, I., Eytan, E., Israel, A., Mercurio, F., Iwai, K., Schwartz, A.L., and Ciechanover, A. (2000). SCF beta-TrcP ubiquitin ligase-mediated processing of NF-kappa B p105 requires phosphorylation of its C-terminus by I kappa B kinase. Embo Journal *19*, 2580-2591.

Ottenheijm, C.A.C., Heunks, L.M.A., Li, Y.P., Jin, B.W., Minnaard, R., van Hees, H.W.H., and Dekhuijzen, P.N.R. (2006). Activation of the ubiquitin-proteasome pathway in the diaphragm in chronic obstructive pulmonary disease. Am J Respir Crit Care Med *174*, 997-1002.

Otulakowski, G., Engelberts, D., Gusarova, G.A., Bhattacharya, J., Post, M., and Kavanagh, B.P. (2014). Hypercapnia attenuates ventilator-induced lung injury via a disintegrin and metalloprotease-17. Journal of Physiology-London *592*, 4507-4521.

Palombella, V.J., Rando, O.J., Goldberg, A.L., and Maniatis, T. (1994). The ubiquitin-proteasome pathway is required for processing the NF-kappa-B1 precursor protein and the activation of NF-kappa-B. Cell *78*, 773-785.

Pangestuti, R. (2009). An Investigation into the Role of the Ubiquitin-Proteasome System in Plant Defence. In Faculty of Biomedical and Life Science (University of Glasgow).

Passmore, L.A., and Barford, D. (2004). Getting into position: the catalytic mechanisms of protein ubiquitylation. Biochem J *379*, 513-525.

Peng, J.M., Schwartz, D., Elias, J.E., Thoreen, C.C., Cheng, D.M., Marsischky, G., Roelofs, J., Finley, D., and Gygi, S.P. (2003). A proteomics approach to understanding protein ubiquitination. Nat Biotechnol *21*, 921-926.

Perkins, N.D. (2007). Integrating cell-signalling pathways with NF-kappa B and IKK function. Nature Reviews Molecular Cell Biology *8*, 49-62.

Petroski, M.D., and Deshaies, R.J. (2005). Function and regulation of Cullin-RING ubiquitin ligases. Nature Reviews Molecular Cell Biology *6*, 9-20.

Pichler, A., Knipscheer, P., Oberhofer, E., van Dijk, W.J., Korner, R., Olsen, J.V., Jentsch, S., Melchior, F., and Sixma, T.K. (2005). SUMO modification of the ubiquitin-conjugating enzyme E2-25K. Nat Struct Mol Biol *12*, 264-269.

Pickart, C.M. (2001). Mechanisms underlying ubiquitination. Annual Review of Biochemistry *70*, 503-533.

Pickart, C.M., and Raasi, S. (2005). Controlled synthesis of polyubiquitin chains. In Ubiquitin and Protein Degradation, Pt B, R.J. Deshaies, ed. (San Diego: Elsevier Academic Press Inc), pp. 21-36.

Puhan, M.A., Gimeno-Santos, E., Scharplatz, M., Troosters, T., Walters, E.H., and Steurer, J. (2011). Pulmonary rehabilitation following exacerbations of chronic obstructive pulmonary disease. The Cochrane database of systematic reviews, Cd005305.

Rappsilber, J., Mann, M., and Ishihama, Y. (2007). Protocol for micro-purification, enrichment, pre-fractionation and storage of peptides for proteomics using StageTips. Nature protocols *2*, 1896-1906.

Rodrigo-Brenni, M.C., Foster, S.A., and Morgan, D.O. (2010). Catalysis of lysine 48-specific ubiquitin chain assembly by residues in E2 and ubiquitin. Mol Cell *39*, 548-559.

Sadowski, M., and Sarcevic, B. (2010). Mechanisms of mono- and poly-ubiquitination: Ubiquitination specificity depends on compatibility between the E2 catalytic core and amino acid residues proximal to the lysine. Cell Div *5*, 5.

Saha, A., Lewis, S., Kleiger, G., Kuhlman, B., and Deshaies, R.J. (2011). Essential role for ubiquitin-ubiquitin-conjugating enzyme interaction in ubiquitin discharge from Cdc34 to substrate. Mol Cell *42*, 75-83.

Singh, S.K., Sahu, I., Mali, S.M., Hemantha, H.P., Kleifeld, O., Glickman, M.H., and Brik, A. (2016). Synthetic Uncleavable Ubiquitinated Proteins Dissect Proteasome Deubiquitination and Degradation, and Highlight Distinctive Fate of Tetraubiquitin. J Am Chem Soc *138*, 16004-16015.

Song, M., Pinsky, M.R., and Kellum, J.A. (2008). Heat shock factor 1 inhibits nuclear factor-kappaB nuclear binding activity during endotoxin tolerance and heat shock. Journal of critical care *23*, 406-415.

Stadie, W.C., and O'Brien, H. (1936). The carbamate equillbrium I. The equilibrium of amino acids, carbon dioxide, and carbamates in aqueous solution; With a note on the Ferguson-Roughton careamate method. Journal of Biological Chemistry *112*, 723-758.

Sun, S.C., Ganchi, P.A., Ballard, D.W., and Greene, W.C. (1993). Nf-kappa-B controls expression of inhibitor I-kappa-B-alpha - evidence for an inducible autoregulatory pathway. Science *259*, 1912-1915.

Supuran, C.T., Scozzafava, A., and Casini, A. (2003). Carbonic anhydrase inhibitors. Medicinal Research Reviews *23*, 146-189.

Suraweera, A., Munch, C., Hanssum, A., and Bertolotti, A. (2012). Failure of amino acid homeostasis causes cell death following proteasome inhibition. Mol Cell *48*, 242-253.

Sznajder, J.I. (2001). Alveolar edema must be cleared for the acute respiratory distress syndrome patient to survive. Am J Respir Crit Care Med *163*, 1293-1294.

Takeshita, K., Suzuki, Y., Nishio, K., Takeuchi, O., Toda, K., Kudo, H., Miyao, N., Ishii, M., Sato, N., Naoki, K.*, et al.* (2003). Hypercapnic acidosis attenuates endotoxin-induced nuclear factor-[kappa]B activation. American journal of respiratory cell and molecular biology *29*, 124-132.

Terrier, P., and Douglas, D.J. (2010). Carbamino Group Formation with Peptides and Proteins Studied by Mass Spectrometry. J Am Soc Mass Spectrom *21*, 1500-1505.

Thrower, J.S., Hoffman, L., Rechsteiner, M., and Pickart, C.M. (2000). Recognition of the polyubiquitin proteolytic signal. Embo Journal *19*, 94-102.

Tomanek, L., Zuzow, M.J., Ivanina, A.V., Beniash, E., and Sokolova, I.M. (2011). Proteomic response to elevated PCO2 level in eastern oysters, Crassostrea virginica: evidence for oxidative stress. J Exp Biol *214*, 1836-1844.

Townsend, P.D., Holliday, P.M., Fenyk, S., Hess, K.C., Gray, M.A., Hodgson, D.R., and Cann, M.J. (2009). Stimulation of mammalian G-protein-responsive adenylyl cyclases by carbon dioxide. The Journal of biological chemistry *284*, 784-791.

Turner, M.J., Saint-Criq, V., Patel, W., Ibrahim, S.H., Verdon, B., Ward, C., Garnett, J.P., Tarran, R., Cann, M.J., and Gray, M.A. (2016). Hypercapnia modulates cAMP signalling and cystic fibrosis transmembrane conductance regulator-dependent anion and fluid secretion in airway epithelia. J Physiol *594*, 1643-1661.

Vadasz, I., Dada, L.A., Briva, A., Helenius, I.T., Sharabi, K., Welch, L.C., Kelly, A.M., Grzesik, B.A., Budinger, G.R.S., Liu, J.*, et al.* (2012). Evolutionary Conserved Role of c-Jun-N-Terminal Kinase in CO_2-Induced Epithelial Dysfunction. PloS one *7*, 9.

Vadasz, I., Dada, L.A., Briva, A., Trejo, H.E., Welch, L.C., Chen, J., Toth, P.T., Lecuona, E., Witters, L.A., Schumacker, P.T.*, et al.* (2008). AMP-activated protein kinase regulates CO_2-induced alveolar epithelial dysfunction in rats and human cells by promoting Na,K-ATPase endocytosis. The Journal of clinical investigation *118*, 752-762.

Vadasz, I., Raviv, S., and Sznajder, J.I. (2007). Alveolar epithelium and Na,K-ATPase in acute lung injury. Intensive care medicine *33*, 1243-1251.

Vandegriff, K.D., Benazzi, L., Ripamonti, M., Perrella, M., Letellier, Y.C., Zegna, A., and Winslow, R.M. (1991). Carbon-dioxide binding to human hemoglobin cross-linked between the alpha-chains. Journal of Biological Chemistry *266*, 2697-2700.

Velentzas, P.D., Velentzas, A.D., Mpakou, V.E., Antonelou, M.H., Margaritis, L.H., Papassideri, I.S., and Stravopodis, D.J. (2013). Detrimental effects of proteasome inhibition activity in Drosophila melanogaster: implication of ER stress, autophagy, and apoptosis. Cell biology and toxicology *29*, 13-37.

Wang, N.Z., Gates, K.L., Trejo, H., Favoreto, S., Schleimer, R.P., Sznajder, J.I., Beitel, G.J., and Sporn, P.H.S. (2010). Elevated CO_2 selectively inhibits interleukin-6 and tumor necrosis factor expression and decreases phagocytosis in the macrophage. Faseb Journal *24*, 2178-2190.

Wauer, T., Swatek, K.N., Wagstaff, J.L., Gladkova, C., Pruneda, J.N., Michel, M.A., Gersch, M., Johnson, C.M., Freund, S.M., and Komander, D. (2015). Ubiquitin Ser65 phosphorylation affects ubiquitin structure, chain assembly and hydrolysis. EMBO J *34*, 307-325.

Welch, L.C., Lecuona, E., Briva, A., Trejo, H.E., Dada, L.A., and Sznajder, J.I. (2010). Extracellular signal-regulated kinase (ERK) participates in the hypercapnia-induced Na,K-ATPase downregulation. FEBS Lett *584*, 3985-3989.

West, J.B. (2014). Joseph Black, carbon dioxide, latent heat, and the beginnings of the discovery of the respiratory gases. Am J Physiol Lung Cell Mol Physiol *306*, L1057-1063.

Wisniewski, J.R., Zougman, A., Nagaraj, N., and Mann, M. (2009). Universal sample preparation method for proteome analysis. Nat Methods *6*, 359-362.

Wu, C., and Ghosh, S. (1999). beta-TrCP mediates the signal-induced ubiquitination of I kappa B beta. Journal of Biological Chemistry *274*, 29591-29594.

Wu, G., Xu, G.Z., Schulman, B.A., Jeffrey, P.D., Harper, J.W., and Pavletich, N.P. (2003). Structure of a beta-TrCP1-Skp1-beta-catenin complex: Destruction motif binding and lysine specificity of the SCF beta-TrCP1 ubiquitin ligase. Molecular Cell *11*, 1445-1456.

Yamaguchi, K., and Hausinger, R.P. (1997). Substitution of the urease active site carbamate by dithiocarbamate and vanadate. Biochemistry *36*, 15118-15122.

Yang, M.J., Chen, T.Y., Li, X.L., Yu, Z., Tang, S.Q., Wang, C., Gu, Y., Liu, Y.F., Xu, S., Li, W.H.*, et al.* (2015). K33-linked polyubiquitination of Zap70 by Nrdp1 controls CD8(+) T cell activation. Nature Immunology *16*, 1253-1262.

Yaron, A., Gonen, H., Alkalay, I., Hatzubai, A., Jung, S., Beyth, S., Mercurio, F., Manning, A.M., Ciechanover, A., and Ben-Neriah, Y. (1997). Inhibition of NF-kappa B cellular function via specific targeting of the I kappa B-ubiquitin ligase. Embo Journal *16*, 6486-6494.

Yaron, A., Hatzubai, A., Davis, M., Lavon, I., Amit, S., Manning, A.M., Andersen, J.S., Mann, M., Mercurio, F., and Ben-Neriah, Y. (1998). Identification of the receptor component of the I kappa B alpha-ubiquitin ligase. Nature *396*, 590-594.

Yuan, W.C., Lee, Y.R., Lin, S.Y., Chang, L.Y., Tan, Y.P., Hung, C.C., Kuo, J.C., Liu, C.H., Lin, M.Y., Xu, M.*, et al.* (2014). K33-Linked Polyubiquitination of Coronin 7 by Cul3-KLHL20 Ubiquitin E3 Ligase Regulates Protein Trafficking. Molecular Cell *54*, 586-600.

Zinngrebe, J., Montinaro, A., Peltzer, N., and Walczak, H. (2014). Ubiquitin in the immune system. EMBO Rep *15*, 28-45.